

**A STUDY ON THE EFFECT OF DIFFERENT CURING REGIMES ON  
PERFORMANCE OF UHPC MIXTURES CONTAINING NATURAL  
POZZOLAN**

BY

**KHALED OWN MOHAISEN**

A Thesis Presented to the  
DEANSHIP OF GRADUATE STUDIES

**KING FAHD UNIVERSITY OF PETROLEUM & MINERALS**

DHAHRAN, SAUDI ARABIA

In Partial Fulfillment of the  
Requirements for the Degree of

**MASTER OF SCIENCE**

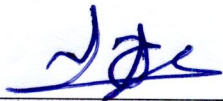
In

**CIVIL ENGINEERING**

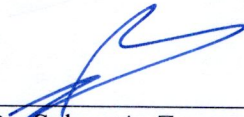
June 2017

KING FAHD UNIVERSITY OF PETROLEUM & MINERALS  
DHAHRAN- 31261, SAUDI ARABIA  
**DEANSHIP OF GRADUATE STUDIES**

This thesis, written by **KHALED OWN MOHAISEN** under the direction his thesis advisor and approved by his thesis committee, has been presented and accepted by the Dean of Graduate Studies, in partial fulfillment of the requirements for the degree of **MASTER OF SCIENCE IN CIVIL ENGINEERING.**



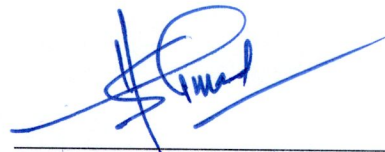
Dr. Salah U. Al-Dulaijan  
Department Chairman



Dr. Salam A. Zummo  
Dean of Graduate Studies

5/6/17

Date



Dr. Shamsad Ahmad  
(Advisor)



Dr. Mohammad Maslehuddin  
(Member)



Dr. Salah U. Al-Dulaijan  
(Member)

© Khaled Own Mohaisen  
2017

To  
My Beloved Parents 'Own and Mona'  
My Lovely Wife 'Shimaa'  
My Brothers and Sisters  
For Their Support, Patience, and Love

## ACKNOWLEDGMENTS

In the Name of Allah the All-Merciful, the Ever Merciful. All perfect praise be to Allah, the Lord of the worlds, for guiding me and granting me patience, knowledge, courage, and health, to complete this research successfully. May the peace and blessings be upon our Prophet Muhammad, upon his household, his companions, and upon those following them in goodness until the Day of Judgment.

I would like to express my love and gratitude to my dear parents, my lovely wife, my adorable brothers and sisters and all my relatives for their support, encouragement, prayers and infinite patience, without them it would be difficult for me to achieve my educational goals.

Acknowledgement is also due to King Fahd University of Petroleum & Minerals and the Civil Engineering department for giving me the opportunity to complete my master degree and providing me the facilities that I need.

I would also like to express my heartfelt gratitude to the people who helped me bring this study into reality. I am very grateful to my advisor Prof. Shamshad Ahmad and my committee members, Prof. Mohammad Maslehuddin Saheb and Dr. Salah U. Al-Dulaijan, for technical support, continuous guidance, suggestions and constructive comments during my research journey.

My special thanks go to my senior colleagues and all friends especially, Eng. Khaled Assi, Eng. Rida Assaggaf and Eng. Saheed Kolawole Adekunle for their support and help in scientific and experimental program.

Finally, thanks to all my friends in KFUPM, especially the Palestinian community for creating the convenient atmosphere that helped us to overcome the homesickness. May Allah continue to help and protect every one of you.

# TABLE OF CONTENTS

ACKNOWLEDGMENTS .....	V
TABLE OF CONTENTS.....	VI
LIST OF TABLES.....	IX
LIST OF FIGURES.....	X
LIST OF ABBREVIATIONS.....	XIII
ABSTRACT .....	XIV
ملخص الرسالة .....	XVI
CHAPTER 1 INTRODUCTION.....	1
1.1 General .....	1
1.2 The Need for This Research.....	3
1.3 Objectives .....	3
CHAPTER 2 LITERATURE REVIEW .....	5
2.1 Background of Ultra-High Performance Concrete.....	5
2.2 Ingredients and Mixture Proportioning of UHPC .....	7
2.3 The Use of Natural Pozzolan in UHPC .....	8
2.4 Accelerated Carbonation Curing Mechanism and Performance .....	9
2.5 Steam Curing .....	11
CHAPTER 3 RESEARCH METHODOLOGY .....	14
3.1 Introduction.....	14
3.2 UHPC Mixtures with Natural Pozzolan.....	14
3.3 Materials.....	16
3.3.1 Powders.....	16

3.3.2 Fine Aggregates.....	17
3.3.3 Superplasticizer (SP) .....	18
3.3.4 Steel Fiber.....	18
3.3.5 CO <sub>2</sub> used for accelerated carbonation curing (ACC) .....	19
3.3.6 Mixing water .....	19
3.4 Design of Selected UHPC Mixtures.....	19
3.5 Procedure for Preparation of UHPC Mixtures .....	20
3.6 Flow Test on Fresh Mixtures of UHPC.....	21
3.7 Casting .....	22
3.8 Curing Regimes.....	22
3.8.1 Burlap curing .....	23
3.8.2 Steam curing.....	23
3.8.3 Accelerated carbonation curing set up.....	26
3.9 Testing of Hardened UHPC Specimens .....	28
3.9.1 Details of the tests for each curing regime .....	28
3.9.2 Compressive strength .....	30
3.9.3 Modulus of elasticity .....	31
3.9.4 Split tensile strength .....	33
3.9.5 Drying shrinkage .....	35
3.9.6 Fracture toughness .....	36
3.9.7 Chloride permeability.....	42
3.9.8 Scanning electron microscopy (SEM).....	43
<b>CHAPTER 4 RESULTS AND DISCUSSIONS .....</b>	<b>45</b>
4.1 Selection of Optimal Duration of Steam Curing (SC) .....	45
4.2 Selection of Optimal Pressure of Accelerated Carbonation Curing (ACC) .....	47
4.3 Workability .....	48
4.4 Compressive Strength.....	50

4.5	Modulus of Elasticity .....	58
4.6	Splitting Tensile Strength.....	60
4.7	Fracture Toughness .....	61
4.8	Chloride Permeability .....	63
4.9	Drying Shrinkage.....	65
4.10	Scanning Electron Micrographs (SEM) and Energy-Dispersive X-ray Spectrographs (EDS) ...	70
<b>CHAPTER 5 CONCLUSIONS AND RECOMMENDATIONS .....</b>		<b>74</b>
5.1	Conclusions.....	74
5.2	Recommendations from this work .....	75
5.3	Recommendations for future work .....	76
<b>REFERENCES.....</b>		<b>77</b>
<b>VITAE .....</b>		<b>83</b>



## LIST OF TABLES

Table 2.1 Compressive strength values of steam cured UHPC .....	12
Table 3.1 Details of UHPC mixtures with different replacements of Portland cement and SF fume by NP .....	15
Table 3.2: Chemical composition of Type I Portland cement. ....	16
Table 3.3: Chemical composition of silica fume (SF). ....	16
Table 3.4: Chemical composition of natural pozzolan (NP).....	17
Table 3.5: Fine aggregate grading (FA).....	17
Table 3.6: Technical data of MasterGlenium51. ....	18
Table 3.7: Steel fiber characteristics. ....	18
Table 3.8: Analysis of CO <sub>2</sub> provided by SIGAS. ....	19
Table 3.9: Proportions of selected UHPC mixtures for one m <sup>3</sup> .....	20
Table 3.10: Details of specimens of various tests per mixture .....	29
Table 4.1: Compressive strength values with and without SC .....	45
Table 4.2: Compressive strength of M0 after 10 h of ACC at different pressures .....	47
Table 4.3: Summarization of curing regime properties .....	48
Table 4.4: Compressive strength results for all SC specimens. ....	51
Table 4.5: Compressive strength results for all ACC specimens.....	52
Table 4.6: Compressive strength results for all BC specimens. ....	52
Table 4.7: Modulus of elasticity results for All UHPC Mixtures .....	58
Table 4.8: Splitting tensile strength for all UHPC mixtures. ....	60
Table 4.9: Fracture toughness parameters for all UHPC mixtures .....	62
Table 4.10: Different chloride permeability categories [52] . ....	63
Table 4.11: Chloride penetration results for all UHPC mixtures.....	64

## LIST OF FIGURES

Figure 2.1: Sherbrooke footbridge, Canada, 1997 .....	6
Figure 2.2: The Peace Bridge in Seoul, South Korea, 2003 .....	6
Figure 3.1: UHPC mixer (MICRONS) .....	20
Figure 3.2: Impact table used to measure the UHPC flow .....	22
Figure 3.3: Specimens under burlap curing .....	23
Figure 3.4: The oven used in SC regime and the water plate .....	24
Figure 3.5: Set-up for the ACC.....	26
Figure 3.6: Schematic diagram of ACC set-up .....	27
Figure 3.7: Preparing of the test specimens .....	30
Figure 3.8: Compressive strength test preparation .....	31
Figure 3.9: Modulus of elasticity test installation.....	32
Figure 3.10: Split tensile strength test installation.....	34
Figure 3.11: Drying shrinkage apparatus and measurements .....	35
Figure 3.12: Details of clip gauge attached to UHPC prisms used to measures the displacement of crack mouth opening (CMOD).....	37
Figure 3.13: Complete test setup for measuring fracture toughness test.. .....	38
Figure 3.14: Loading and unloading compliance $C_i$ and $C_u$ .....	41
Figure 3.15: Fracture toughness specimen's preparation, installation and testing .....	44
Figure 3.16: Chloride permeability test machine and sample preparation .....	44
Figure 3.17: Scanning electron microscope.....	44
Figure 4.1: Compressive strength of UHPC mixtures under SC .....	46
Figure 4.2: Compressive strength values at different SC periods.....	47
Figure 4.3: Compressive strength results at different $CO_2$ pressures .....	48

Figure 4.4: Decrease in flow with increase in level of replacement of MS by NP.....	49
Figure 4.5: Decrease in flow with increase in level of replacement of cement by NP .....	50
Figure 4.6: Compressive strength of UHPC mixture M0 subjected to different curing regimes .....	53
Figure 4.7: Compressive strength of UHPC mixture M1 subjected to different curing regimes .....	55
Figure 4.8: Compressive strength of UHPC mixture M2 subjected to different curing regimes .....	56
Figure 4.9: Compressive strength of UHPC mixture M3 subjected to different curing regimes .....	56
Figure 4.10: Compressive strength of UHPC mixture M4 subjected to different curing regimes .....	57
Figure 4.11: Compressive strength of UHPC mixture M5 subjected to different curing regimes .....	57
Figure 4.12: Modulus of elasticity of All UHPC Mixtures .....	58
Figure 4.13: Stress-Strain responses for M0 with different curing regimes .....	59
Figure 4.14: Splitting tensile strength for all UHPC mixtures .....	61
Figure 4.15: $K_{ic}$ values for all UHPC mixtures.....	62
Figure 4.16: Chloride permeability results for all UHPC mixtures.....	64
Figure 4.17: Drying shrinkage strain for mixture M0.....	66
Figure 4.18: Drying shrinkage strain for mixture M1.....	66
Figure 4.19: Drying shrinkage strain for mixture M2.....	67
Figure 4.20: Drying shrinkage strain for mixture M3.....	67
Figure 4.21: Drying shrinkage strain for mixture M4.....	68
Figure 4.22: Drying shrinkage strain for mixture M5.....	68
Figure 4.23: 7-days drying shrinkage readings.....	69

Figure 4.24: Ultimate Drying Shrinkage Values for All UHPC Mixtures .....	69
Figure 4.25: SEM micrograph of the mixture M0-SC .....	70
Figure 4.26: EDS of the mixture M0-SC .....	70
Figure 4.27: SEM micrograph of the mixture M0-ACC.....	70
Figure 4.28: EDS of the mixture M0-ACC.....	70
Figure 4.29: SEM micrograph of the mixture M0-BC. ....	70
Figure 4.30: EDS of the mixture M0-BC.....	70

## **LIST OF ABBREVIATIONS**

<b>UHPC</b>	:	Ultra-High Performance Concrete
<b>SC</b>	:	Steam Curing
<b>ACC</b>	:	Accelerated Carbonation Curing
<b>BC</b>	:	Burlap Curing
<b>OPC</b>	:	Ordinary Portland Cement

## **ABSTRACT**

**Full Name : Khaled Own Awad Mohaisen**  
**Thesis Title : A Study on the Effect of Different Curing Regimes on Performance of UHPC Mixtures Containing Natural Pozzolan**  
**Major Field : Civil Engineering (Structures)**  
**Date of Degree : June 2017**

Ultra-high performance concrete (UHPC) is a new generation of concrete that has been developed recently. Because of denser microstructure and presence of fibers, UHPC has excellent properties like very high strength, elasticity, ductility, long-term stability, and durability. Attempts have been made to develop new UHPC mixtures using different alternative materials and curing regimes to control the heat of hydration, to reduce the overall cost, and to achieve environmental benefits. Natural pozzolan (NP) that is a siliceous or siliceous and aluminous material without considerable lime can be used for partially replacing the Portland cement and silica fume resulting in lower cost of production of UHPC. In addition, the utilization of NP for reducing consumption of cement would make the UHPC an environmental friendly material by reducing the emission of carbon dioxide. Different curing regimes, such as accelerated carbonation curing (ACC) and steam curing (SC) should be tried for improving the performance of UHPC containing NP. ACC is a newly developed method of concrete curing that consists of forcing carbon dioxide gas to penetrate fresh concrete under optimum pressure and exposure duration. ACC method has economic and environmental benefits, such as reducing CO<sub>2</sub> emission problems in the air.

In this study, several mixtures of UHPC were considered by selecting various combinations of the partial replacements of Portland cement and silica fume by NP. Each mixture was subjected to three curing regimes, which included burlap curing (BC), ACC and SC. The

cured specimens of the UHPC mixtures were tested to determine, mechanical properties (compressive and tensile strengths, modulus of elasticity, and fracture toughness), shrinkage, durability characteristics (chloride permeability), and the morphological characteristics (SEM). The test results were utilized to evaluate the effects of the incorporation of NP and curing regimes on the performance of UHPC. It indicates that the NP can be successfully used to replace the silica fume and Portland cement up to 50 and 30%, respectively, without compromising with the required quality of the UHPC mixtures. The performance of SC regime was found to be better than that of BC and ACC regimes. It is very interesting to note that the UHPC mixtures subjected to ACC and BC regimes performed almost in the similar way providing to use these two curing regimes alternatively depending on the situation.

## ملخص الرسالة

الاسم الكامل: خالد عون عوض محيسن

عنوان الرسالة: دراسة حول تأثير طرق المعالجة المختلفة على كفاءة الخرسانة عالية الاجهاد المحتوية على البوزولان الطبيعي

التخصص: الهندسة المدنية

تاريخ الدرجة العلمية: يونيو 2017

الخرسانة عالية الاجهاد هي نوع جديد متطور من الخرسانة والذي تم تطويره حديثا. بسبب بنيته المجهرية ذات الكثافة العالية ووجود ألياف الحديد فيه. الخرسانة عالية الأداء لها خصائص ومزايا عديدة مثل امتلاكها لقوة وصلابة عالية , تماسك أكبر , احتوائها على نسبة قليلة جدا من المسامات , وصمودها لفترة أطول ضد التأثيرات الجوية المختلفة. عدة محاولات تمت لتطوير الخرسانة عالية الأداء باستخدام مواد محلية رخيصة الثمن لتقليل التكلفة وجعلها صديقة للبيئة. البوزولان الطبيعي والذي هو عبارة عن مواد سيليكية او سيليكية وألمونية ونسبة قليلة جدا من الجير يمكن استخدامه كبديل جزئي عن الاسمنت والسليكا بحيث يقلل من التكلفة الكلية للخرسانة بدون تأثير واضح على قوة تحمل الخرسانة وبالتالي يقلل من استهلاك الاسمنت والذي بدوره يجعل الخرسانة صديقة للبيئة من حيث استخدام نسبة أقل من الاسمنت الذي ينتج كميات كبيرة من ثاني اكسيد الكربون. طرق معالجة معجلة مختلفة باستخدام (بخار الماء , ثاني أكسيد الكربون) تم استخدامها بغرض الوصول للقوة القصوى خلال أقل زمن لتسريع العمل واستخدام الخرسانة في أسرع وقت ممكن وبالأخص في مصانع الخرسانة مسبقة الصب. المعالجة المعجلة باستخدام بخار الماء هي احدى الطرق المستخدمة للحصول على قوة مبكرة للخرسانة لتوفير الوقت وبالذات في مجال صناعة الخرسانة مسبقة الصب وهي احدى الطرق التي سوف يتم استخدامها, الطريقة الثانية في المعالجة باستخدام ثاني اكسيد الكربون وهي من طرق المعالجة المستخدمة حديثا في هذا المجال حيث يتم تعريض العينات لضغط غاز ثاني أكسيد الكربون وتتميز هذه الطريقة بانها طريقة اقتصادية وصديقة للبيئة حيث يتم جمع غاز ثاني اكسيد الكربون الناتج من انتاج الاسمنت واعادة ضخه للعينات لزيادة قوته وتقليل انبعاثات الكربون.



عدة خلطات تم عملها بنسب خلط متفاوتة باستبدال البوزولان الطبيعي بالاسمنت والسيليكا كل على حدى بغرض الوصول لأفضل خلطة من حيث الكفاءة والاقتصادية, ومن ثم معالجة الخلطات المختارة بثلاث طرق معالجة مختلفة, وعمل فحوصات المتانة والتركيب الجزيئي والخصائص الميكانيكية (كالصلابة ومعامل المرونة وقدرة الشد والضغط) وذلك لاختيار النسبة الأفضل ليتم استخدامها في قطاع الخرسانة مسبقة الصب عالية الاجهاد في المملكة العربية السعودية لتوفير الوقت والجهد والمحافظة على البيئة في الوقت ذاته. تشير نتائج فحوصات تأثير وجود البوزولان الطبيعي مع طرق المعالجة المختلفة على الخرسانة عالية الأداء أنه يمكن استبدال الاسمنت والسيليكا بالبوزولان الطبيعي في الخرسانة عالية الأداء بنجاح بنسبة 50 و 30% للاسمنت والسيليكا على التوالي, وبدون تأثير ملاحظ على كفاءة الخرسانة عالية الأداء.

كان أداء طريقة المعالجة باستخدام بخار الماء أفضل من طريقة المعالجة باستخدام ثاني أكسيد الكربون والمعالجة التقليدية باستخدام الماء. ومن الجدير بالذكر أن أداء الخرسانة عالية الأداء التي تمت معالجتها باستخدام ثاني أكسيد الكربون والمعالجة التقليدية برش الماء كانت متقاربة الى حد كبير وبالتالي يمكن استخدام كلا الطريقتين حسب الحالة.

# CHAPTER 1

## INTRODUCTION

### 1.1 General

Ultra-High Performance Concrete (UHPC), is an innovative generation of concrete technology material developed in 1990s in France [1]. It is a new generation of concrete developed to improve the mechanical properties along with durability than normal and high-performance concretes. This improvement is achieved by limiting water to cement ratio on a very low side ( $< 0.20$ ), eliminating coarse aggregate, using fine quartz sand, adding high dosages of cementitious materials and superplasticizer, implementing high pressure and high temperature curing regimes, also using fibers to enhance the tensile strength, toughness and ductility of UHPC [2].

A series of UHPC mixtures having wide ranges of mechanical and durability properties can be produced by selecting different possible materials, mix proportions, and curing regimes. Although the production cost of an UHPC mixture can be very high as compared to the normal-strength concrete, due to its high mechanical performance and long service life without the need for repairing makes it affordable. Nevertheless, it is possible to reduce the cost of the UHPC by using cheaper and locally available alternative materials and curing methods.

The cementitious materials used in UHPC consist of the blend of Portland cement and mineral admixtures. Silica fume is used as a common mineral admixture in the UHPC mixtures. The use of a high amount of Portland cement in the UHPC has two negative impacts. First, it increases the unit cost and secondly, the high consumption of cement is associated with the generation of carbon dioxide that leads to the environmental problems. Furthermore, since the silica fume is not a cheaply available in Saudi Arabia, its high consumption in UHPC will make the UHPC costlier. Therefore, there is a need for exploring possibility of using a cheaply and abundantly available mineral admixture for partially replacing the Portland cement and silica fume.

Recently, various mineral admixtures have been tried to partially replace Portland cement and silica fume in the UHPC mixtures. Some examples include the use of fly ash, limestone powder, natural pozzolan, etc. Natural pozzolan has low cost and readily available in Saudi Arabia, which has potential to be used as mineral admixtures in concrete [3]. Recently, many studies considered partial replacement of cement by natural pozzolan to achieve an improvement in the strength and durability [4-6]. Al-Chaar mentioned that cement with pozzolan has lower heat of hydration, which enhance concrete workability and durability, it also has a good effect to resists sulfate attack and alkali silica reactions [6].

Accelerated curing of concrete is used to yield high early age strength concrete compared with traditional methods, which minimize the cost required by reducing the time needed. Various accelerated curing regimes have been used for UHPC, such as steam curing, curing at high temperature with water vapor [7 and 8]. It is noticed that curing concrete under high temperature and humidity will enhance the microstructure of the concrete in short time. In addition, mechanical properties and long-term durability [9]. Recently, carbonation curing

is emerging as one of the accelerated curing methods of concrete. The accelerated carbonation curing (ACC) is found effective in improving the physico-mechanical properties and durability of concrete as it increases the density, strength, modulus of elasticity, sulfate resistance, freeze-thaw resistance and decreases the water absorption and chloride ion penetration [10-14].

## **1.2 The Need for This Research**

The technical, environmental and economic benefits associated with the use of natural pozzolan in UHPC as a partial replacement of cementitious materials and the considerable effect of the different curing regimes on quality of such concrete provides an opportunity to explore the possibility of producing UHPC with alternative cementitious materials and curing regimes. Accordingly, the proposed study is needed to select optimal mixtures of UHPC with suitable curing regimes by considering different possible combinations of partial replacement of cement and silica fume by natural pozzolan and three different curing regimes.

## **1.3 Objectives**

The main objective of the present study was to investigate the effectiveness of using natural pozzolan material as a partial replacement of cement and silica fume in producing UHPC using different curing regimes.

The specific objectives are the following:

- (i) Design the mixtures of UHPC considering different possible dosages of natural pozzolan for partially replacing the cement and silica fume,

- (ii) Evaluate performance of different curing regimes (normal burlap curing, accelerated carbonation curing, and steam curing) for curing each selected UHPC mixture, and
- (iii) Select optimum mixtures of UHPC and suitable curing regime based on the evaluation of performance in terms of the mechanical and durability properties of UHPC mixtures produced with different dosages of natural pozzolan and cured using different curing regimes.

## **CHAPTER 2**

### **LITERATURE REVIEW**

A review of literature pertaining to the background of UHPC, the ingredients and mixture proportioning of UHPC, use of natural pozzolan in UHPC as a partial replacer of Portland cement and silica fume, and various curing regimes suitable for UHPC are presented in the following sections.

#### **2.1 Background of Ultra-High Performance Concrete**

During the last three decades, wonderful progress has been made in concrete technology. One of the revolutions is the development of ultra-high-performance concrete (UHPC) with its incredible mechanical properties (very high strength, elasticity and ductility) and a remarkable increase in the durability performance. A mixture of UHPC possesses compressive strength above 150 MPa [15]. Many patented mixtures of UHPC emerged out that included Ductal, Ceracem and BCV [1]. Ductal is the most common type of patented UHPC mixture launched by Lafarge company in North America [7] that is commercially available globally. As mentioned earlier, a mixture of UHPC consists of cement, fine quartz sand, silica fume, superplasticizer, water, and fibers [16].

UHPC was used for the first time in special applications in the security industry – like vaults, strong rooms and protective defense constructions in Denmark [15]. Then it used in different applications like precast elements for bridge decks; in situ applications for the rehabilitation of deteriorated concrete bridges and industrial floors like Sherbrooke

footbridge, constructed twenty years ago in 1997 in Canada shown in Figure 2.1, and the Peace footbridge in South Korea shown in Figure 2.2 [1].



**Figure 0.1: Sherbrooke footbridge, Canada, 1997**



**Figure 2.2: The Peace Bridge in Seoul, South Korea, 2003**

## 2.2 Ingredients and Mixture Proportioning of UHPC

A high quantity of Portland cement, a high amount of silica fume (with particle size ranging between 0.1 and 1  $\mu\text{m}$ ), a high dosage of superplasticizer, very fine quartz sand (with particle size ranging from 0.15 to 0.60 mm), quartz powder (with particle size smaller than 10  $\mu\text{m}$ ), and fibers are used for producing UHPC mixtures, eliminating the need for the coarse aggregate [17 – 19]. The excellent performance of UHPC is mainly due to its dense microstructure, which is achieved by replacing the coarse aggregate by fine quartz sand that maintains the homogeneity between the cement matrix and the fine aggregate particles [20]. In production of UHPC, the requirement of Portland cement and silica fume may be as high as 1000 and 300  $\text{kg/m}^3$ , respectively, due to increased surface area by using very fine particles of sand and quartz powder [17 and 21].

Following key points regarding proportioning of the UHPC mixtures are noted from the literature [17 and 22 – 26]:

- (i) Maintaining a low water-to-cementitious materials ratio below 0.20 (by mass)
- (ii) Admixing a mineral admixture, usually, silica fume in the range of 15 to 30% by the mass of cement
- (iii) Using a high dosage of superplasticizer, usually above 2.5% by mass of total cementitious materials to achieve a flow in the range of  $200 \pm 20$  mm
- (iv) Using optimum particle size distribution for maximum packing of the particles
- (v) Adding steel fibers in quantity about 6% by mass of UHPC, to enhance ductility, and
- (vi) Adopting a suitable curing regime, which would enable to achieve maximum evolution of the strength.



Ahmad et al. [27] developed an optimum mixture of UHPC using the local materials available in Saudi Arabia. They used fine dune sand obtained from the deserts of Saudi Arabia. Their optimum mixture of UHPC had the following composition:

- Portland cement content: 900 kg/m<sup>3</sup>
- Silica fume content: 220 kg/m<sup>3</sup>
- Water content: 163 kg/m<sup>3</sup>
- Fine dune sand content: 1005 kg/m<sup>3</sup>
- Glenium® 51 superplasticizer content: 40 kg/m<sup>3</sup>
- Steel fiber content: 157 kg/m<sup>3</sup>

The evaluation of the above optimum mixture of UHPC indicated an excellent performance in terms of its flowability, mechanical properties and durability characteristics. In the present study, this mixture is taken as the reference for producing other alternative UHPC mixtures with the provision of replacing the Portland cement and silica fume partially by the natural pozzolan locally available in Saudi Arabia.

### **2.3 The Use of Natural Pozzolan in UHPC**

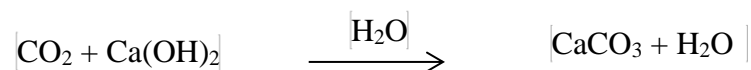
The natural pozzolan has been used for long time (since the Roman ages) as a cementitious material. It is used in concrete due to its good performance and economy [4 and 28]. Like the other mineral admixtures, natural pozzolan when admixed with the Portland cement can adapt the kinetic of hydration, decrease the heat evolution and produce additional C-S-H hydrates [29]. Natural pozzolan influences the cement hydration in a secondary reaction and minimizes the negative effect caused by high temperatures according to its characteristics and the replacement rates in the mixtures. Natural pozzolan gives to the concrete extra performance specially in hot weather conditions, in which the dangerous

effect of the temperature is slightly reduced by the secondary pozzolanic reaction [28]. Among the other mineral admixtures used in concrete, the natural pozzolan can be used most economically due to its availability in Saudi Arabia [3].

Because of its rough particle size, the natural pozzolan slightly reduces the workability of concrete [30]. However, it fills the empty pores between cement particles and other pozzolanic particles [31]. Shannag [30] mentioned that natural pozzolan could be added up to 25% by weight of the cement without decreasing the strength of specimens at 28 days. He also mentioned that higher replacement of about 35% could match the strength of Portland cement at 90 days. Ahmad et al. [32] used the Saudi natural pozzolan in producing UHPC. They reported an acceptable flow and a 28-d water cured compressive strength above 150 MPa when the silica fume was partially replaced by the natural pozzolan. However, they did not try to replace the Portland cement by natural pozzolan for producing the UHPC mixtures.

## 2.4 Accelerated Carbonation Curing Mechanism and Performance

Accelerated carbonation curing is a curing regime in which carbon dioxide gas (CO<sub>2</sub>) sequestration applied on concrete elements during their production. The CO<sub>2</sub> sequestered into concrete reacts with calcium compounds in cement resulting into formation of stable calcium carbonates (CaCO<sub>3</sub>) as described in the following equation [33 and 34].



The CaCO<sub>3</sub> formed as a result of reaction between carbon dioxide and calcium hydroxide reacts with calcium-silicate-hydrate gel (C-S-H) in a secondary reaction which provides a

new gel structure better than that provided by conventional C-S-H [13]. Accelerated carbonation curing method ACC is found to change mainly the microstructure of concrete in addition to concrete mineralogy and morphology. Accelerated carbonation curing leads to the following developments:

- (i) Increase in the concrete density which provides higher strength and durability than the case of conventional curing method [12 and 14].
- (ii) It can lower the pH of concrete by reducing the amount of  $\text{Ca(OH)}_2$ , however, the reduction in pH may not go below threshold value of 10 for initiation of reinforcement corrosion. Furthermore, the acid and sulfate resistance of concrete can be increased due to the reduction in the amount of  $\text{Ca(OH)}_2$ . Therefore, the accelerated carbonation curing can be applied to produce plain as well as reinforced precast concrete components [12 and 35].
- (iii) Decrease in the time required for curing compared with the conventional methods. If the accelerated carbonation curing is adopted in a proper way, the technical and environmental benefits can be achieved as it helps in increasing strength and durability and in reducing the carbon footprint, which is a negative environmental concern associated with cement and concrete industries.

Concentration of  $\text{CO}_2$  injected to the chamber is observed as highly influential factor. Researchers have tried several different  $\text{CO}_2$  concentrations in the range of 14 to 25% for simulating the captured flue gas and used 100%  $\text{CO}_2$  concentration simulating the pure  $\text{CO}_2$  [11 and 36]. Different pressure values have been applied inside the curing chamber by researchers between 1.45 and 72.5 psi. Also, researchers used different exposure durations to  $\text{CO}_2$  gas [11]. Monkman and Shao [37] achieved  $\text{CO}_2$  uptake in the range of 8

to 10% by the mass of binder and reported strength after 2 hours of carbonation curing equal to 80% of the strength of 24 hour conventional curing. Baojian [36] conducted a study on accelerated carbonation curing using recovered CO<sub>2</sub> (100% concentration of CO<sub>2</sub>) maintaining a pressure of 1 bar (0.1 MPa), temperature in the range of about 26 to 30 °C and relative humidity in the range of about 82 to 95 % for a period of 6, 12 and 24 hour. They found an increase in the CO<sub>2</sub> uptake and strength and decrease in drying shrinkage by increasing the duration of the accelerated carbonation curing.

Rostami [13] stated that keeping specimens in the air for some time before exposure to CO<sub>2</sub> gas is very important to allow diffusion of CO<sub>2</sub> into concrete. Kashef-Haghighi and Ghoshal [33 and 38] have observed that the CO<sub>2</sub> uptake is adversely affected by the formation of the layer of CaCO<sub>3</sub>(s) during carbonation because the layer of CaCO<sub>3</sub>(s) decreases the reactive surface area of cement. They also have found that the CO<sub>2</sub> uptake can be increased insignificantly either by using cements having higher amount of reactive mineral or cements having more fineness which would provide a higher reactive surface area [38]. However, evaluating the performance of UHPC mixtures exposed to accelerated carbonation curing would be of a great interest, which was considered in the present research.

## **2.5 Steam Curing**

In precast concrete industries, curing with elevated temperature with relative humidity techniques has been used to gain dense microstructure that provides high early strength and enhanced durability of concrete [9]. Several investigators [29, 39, and 40] reported that the high temperature improves the early strengths of the mixture. Mirza et al. [41] found that blending OPC with pozzolanic materials helps to improve the performance of mortars and

concrete strength on exposure to higher temperature than normal. After the development of UHPC with its excellent properties, many researchers tried to apply various accelerated curing regimes to achieve higher and better properties, especially steam curing because of its excellent effect on the performance of concrete.

Steam curing regime is needed for proper improvement of the microstructure of calcium silicate hydrates (C-S-H) in UHPC mixtures. Prem et al. [8] studied the compressive strength and different microstructure properties of UHPC exposed to an elevated temperature of 100°C with relative humidity of 95% for 18 h. Table 2.1 shows the compressive strength values at different testing ages. In addition, an enhancement in tensile strength observed due to addition of steel fibers in UHPC mixtures. A tensile strength of 11 MPa was observed in UHPC mixes without steel fibers, while a remarkable increase in tensile strength values (18 – 23.8) MPa was noticed as a result of adding steel fibers with different percentages [8].

**Table 2.1: Compressive strength values of steam cured UHPC**

<b>Age at testing day</b>	<b>Compressive strength MPa</b>
3	53
7	120
14	128
28	142

Another study is reported by Ahlborn [7] on UHPC subjected to thermal steam curing. The specimens were subjected to steam treatment at 90° C temperature and a relative humidity of 100% with a total cured time of 48 h. A compressive strength of 214 MPa after 28 days was reported. The modulus of elasticity of the same UHPC mixture after 28 days was

determined as 56 GPa. Moreover, the study showed a negligible value of chloride permeability (15 coulombs) after 28 days of steam curing [7]. Other researchers observed that it is possible to get a compressive strength value of 200 MPa with Young's modulus of 66 GPa. In addition, they showed that the average flexural strength for their standardized specimens is 32 MPa [42]. Moreover, it has been found that the drying shrinkage of 28-day water curing of UHPC specimens was 300 microns, and almost 0.1% water absorption, which is considered as a negligible value [43].

## **CHAPTER 3**

### **RESEARCH METHODOLOGY**

#### **3.1 Introduction**

In this chapter, the research methodology is described highlighting the various aspects of experimental work. Details of the mixtures of UHPC considered with different levels of replacement of Portland cement and silica fume by natural pozzolan are first presented. This is followed by the description of materials used, design of the selected mixtures, procedure for preparation of the UHPC mixtures, flow test of fresh UHPC mixtures, casting procedure, curing regimes, and testing of the specimens for evaluation.

#### **3.2 UHPC Mixtures with Natural Pozzolan**

The optimum mixture of UHPC developed by Ahmad et al. [27] at KFUPM using local fine dune sand, as detailed below, was used as a reference UHPC mixture (M0) for replacing Portland cement and silica fume partially by natural pozzolan with different possible ratios.

- Portland cement content: 900 kg/m<sup>3</sup>
- Silica fume content: 220 kg/m<sup>3</sup>
- Water content: 163 kg/m<sup>3</sup>
- Fine dune sand content: 1005 kg/m<sup>3</sup>
- Glenium<sup>®</sup> 51 superplasticizer content: 40 kg/m<sup>3</sup>
- Steel fiber content: 157 kg/m<sup>3</sup>

To decide the maximum levels of replacement of Portland cement and silica fume by natural pozzolan, several trial mixtures of UHPC were prepared and tested for flow. Based on the minimum required flow of about 180 mm, the maximum limits of the partial replacement of Portland cement and silica fume by natural pozzolan were found to be 30% and 50%, respectively. Two levels of silica fume replacement (25 and 50%) and three levels of Portland cement (10, 20 and 30%) were used. This way a total of five UHPC mixtures, two with partial replacement of silica fume (M1 and M2) and three with Portland cement replacement (M3, M4, and M5) were considered for evaluation of the performance after exposure to different curing regimes.

The details of partial replacements of cement and silica fume (SF) by natural pozzolan (NP) are presented in **Error! Reference source not found..**

**Table 3.1: Details of UHPC mixtures with different replacements of Portland cement and SF fume by NP**

Mixture ID	Replacement	Cement (%)	MS (%)	NP (%)
M0 (Reference)	No replacement	100	100	0
M1	Replacement of MS by NP	100	75	25
M2		100	50	50
M3	Replacement of cement by NP	90	100	10
M4		80	100	20
M5		70	100	30



### 3.3 Materials

#### 3.3.1 Powders

##### (i) Cement

ASTM C 150 Type I Portland cement (OPC) with a specific gravity of 3.15 was used in this study. Table 3.2 shows the chemical composition of cement used in the present study.

**Table 3.2: Chemical composition of type I Portland cement.**

<i>Oxide composition</i>	
<b>Component</b>	<b>Weight %</b>
CaO	64.35
SiO <sub>2</sub>	22.00
Al <sub>2</sub> O <sub>3</sub>	5.64
Fe <sub>2</sub> O <sub>3</sub>	3.80
K <sub>2</sub> O	0.36
MgO	2.11
Na <sub>2</sub> O	0.19
Equivalent alkalis	0.33
SO <sub>3</sub>	2.10
LOI	0.70

##### (ii) Silica Fume (SF)

Silica fume available in the local market was used with the chemical composition shown in Table 3.3.

**Table 3.3: Chemical composition of silica fume (SF).**

<b>Component</b>	<b>Weight %</b>
CaO	0.48
SiO <sub>2</sub>	92.5
Al <sub>2</sub> O <sub>3</sub>	0.72
Fe <sub>2</sub> O <sub>3</sub>	0.96
K <sub>2</sub> O	0.84
MgO	1.78
Na <sub>2</sub> O	0.5
LOI	1.55

### (iii) Natural pozzolan

The natural pozzolan (NP) used was obtained from volcanic rocks in Western areas of Saudi Arabia. It has a specific gravity of 3.00. Table 3.4 shows the chemical composition of the NP used.

**Table 3.4: Chemical composition of natural pozzolan (NP).**

Component	Weight %
CaO	8.06
SiO <sub>2</sub>	42.13
Al <sub>2</sub> O <sub>3</sub>	15.33
Fe <sub>2</sub> O <sub>3</sub>	12.21
K <sub>2</sub> O	0.84
MgO	8.50
Na <sub>2</sub> O	2.99
Na <sub>2</sub> O+(0.658 K <sub>2</sub> O)	3.54
Moisture	0.17

### 3.3.2 Fine Aggregates

Local fine dune sand with water absorption of 0.4% and specific gravity of 2.65 was used as the aggregate in all UHPC mixtures. Grading of the dune sand is shown in Table 3.5.

**Table 3.5: Fine aggregate grading (FA).**

Sieve #	Size	% passing
4	4.75 mm	100
8	2.36 mm	100
16	1.18 mm	100
30	600 µm	76
50	300 µm	10
100	150 µm	4

### 3.3.3 Superplasticizer (SP)

The superplasticizer used in the mixtures was MasterGlenium51®. It was brought from a local manufacture in the Saudi Arabia (BASF Co.). Table 3.6 describes the characteristics of SP as obtained from the supplier company BASF.

**Table 3.6: Technical data of MasterGlenium51.**

Property	explanation
Appearance	Brown liquid
Specific gravity @ 20°C	1.08±0.02 g/cm <sup>3</sup>
pH-value @ 20°C	7.0±1.0
Alkali content	≤ 5.0
Chloride content	≤ 0.1 %

### 3.3.4 Steel Fiber

Steel fibers imported from China with the following properties were used. Table 3.7 shows the properties of the steel fibers as provided by the supplier.

**Table 3.7: Steel fiber characteristics.**

Property	explanation
Type	Smooth plain copper coated steel fibers
Diameter	0.22 mm
Length	13 mm
Aspect ratio	59
Tensile strength	2500 MPa

### 3.3.5 *CO<sub>2</sub> used for accelerated carbonation curing (ACC)*

CO<sub>2</sub> with a high purity of 99.9% was utilized to cure concrete specimens under a constant pressure for required duration. CO<sub>2</sub> gas was sourced from the Saudi Industrial Gas Company (SIGAS). Table 3.8 shows the details of the CO<sub>2</sub> analysis results, as provided by SIGAS.

**Table 3.8: Analysis of CO<sub>2</sub> provided by SIGAS.**

<b>Component</b>	<b>Limit</b>	<b>Act.</b>
Assay	$\geq 99.8\%$	99.9%
CO	<10 ppm	<10 ppm
NO	<2.5 ppm	<2.5 ppm
SO <sub>2</sub>	<0.5 ppm	<0.5 ppm
NO <sub>2</sub>	<2.5 ppm	<2.5 ppm
Water	<32 ppm	<32 ppm
H <sub>2</sub> S	<0.5 ppm	<0.5 ppm

### 3.3.6 *Mixing water*

Normal sweet water was used for mixing, steam curing and burlap curing of the UHPC specimens.

## 3.4 Design of Selected UHPC Mixtures

All the UHPC mixtures considered in this study were designed using absolute volume method based on the physical properties of the ingredients, for example specific gravity. The quantities of ingredients calculated for producing one cubic meter of the each of the UHPC mixtures are presented in Table 3.9.

**Table 3.9: Proportions of selected UHPC mixtures for one m<sup>3</sup>**  
**(Water/binder = 0.145 for all mixtures)**

Ingredients	M0 (Reference)	M1	M2	M3	M4	M5
Cement (kg)	900	900	900	810	720	630
SF (kg)	220	165	110	220	220	220
NP (kg)	0	55	110	90	180	270
Water (kg)	163	163	163	163	163	163
Superplasticizer (kg)	40	40	40	40	40	40
Steel fibers (kg)	157	157	157	157	157	157
Sand (kg)	1005	1021	1036	1002	998	994

### 3.5 Procedure for Preparation of UHPC Mixtures

Mixing of UHPC requires special equipment and procedures to maintain consistency in batching, casting, and curing. A high shear capacity mixer along with vibratory table is required to carry out mixing of the ingredients of UHPC mixtures. In the present work, mixing of UHPC was carried out using MICRONS mixer, as shown in Figure 3.1.



**Figure 3.1: UHPC mixer (MICRONS)**

Following mixing procedure for UHPC was adopted:

- Weigh all constituent materials.
- Add the superplasticizer to water and mix it carefully.
- Place powder materials and sand in mixer pan and mix till a homogenous mixture is obtained, it will take approximately 2 minutes.
- Add two third of the water with superplasticizer slowly.
- Mix for 10-15 minutes until the powder becomes granules.
- Then add the rest of the water with superplasticizer.
- Continue mixing till the mix is completely homogenous and fluid. The time required for this process is about 7-10 minutes, but it can vary a bit due to different ingredients.
- Add the fibers to the mix slowly in small amounts over the course of the next three minutes.
- After the fibers are added, continue running mixer for further three minutes to ensure that the fibers are well dispersed.

It is worth mentioning that the total time of mixing of UHPC varies between 25- 35 minutes. It should be noted that this mixing time is relative and is only specifically applicable to the pan mixer used in this study.

### **3.6 Flow Test on Fresh Mixtures of UHPC**

As soon as mixing was completed, UHPC mixture was tested for consistency. ASTM C 1437 standard test method for measuring flow of hydraulic cement was used to comply with the recommendations (Operating Procedure – Flow Test). In flow test, mini slump cone was filled with UHPC mixture, and then removed slowly to allow the mixture to flow

on the table, then the flow table raised and dropped 20 times and the average diameter of mixtures spread was recorded as flow value. Figure 3.2 shows the flow table that was used to measure the flow of different UHPC mixtures.



**Figure 3.2: Impact table used to measure the UHPC flow**

### **3.7 Casting**

After completion of mixing process, the mixtures were cast into molds within 20 minutes by pouring the material into the molds placed on a vibrating table. The molds filled with the UHPC mixture were vibrated for about 10-20 seconds after filling the whole mold to consolidate the mixture. The specimens in molds were covered with plastic sheets to prevent moisture loss [44].

### **3.8 Curing Regimes**

Each mixture was cured by three types of curing regimes that included traditional burlap curing (BC), steam curing (SC), and accelerated carbonation curing (ACC). The specimens were kept in the molds for a duration of six hours before demolding them and starting the curing, so that they can gain some strength before curing.

### 3.8.1 Burlap curing

The UHPC specimens were subjected to burlap curing by covering them with jute sheets and then sprinkling water over it once in a day. The specimens under burlap curing are shown in Figure 3.3.



**Figure 3.3: Specimens under burlap curing**

### 3.8.2 Steam curing

For steam curing, two major factors are important, temperature and relative humidity. Based on the recommendations of the researchers [7, 8], the steam curing was carried out



at a temperature of 85 °C and a relative humidity of 95%. This curing condition was created inside an oven in which the specimens were stacked above a tray containing water, as shown in Figure 3.4. The required temperature and humidity (i.e., steam) was generated by elevating the temperature of the oven. The water in the tray, upon heating, was converted into water vapor, which was used to cure the specimens.



**Figure 3.4: The oven used in SC regime and the water plate**

The systematic procedure used for steam curing of the UHPC specimens is as follows:

- An oven was used as shown in Figure 3.4. It consisted of a fan to distribute the heat and humidity all around the space inside the oven.
- After keeping the specimens in the oven, it was closed and heating was started. The targeted temperature of 85°C was achieved within 20 min. A temperature sensor was used to check the temperature inside the oven.
- The water in the tray generated the relative humidity. A hygrometer was used for humidity measurements.

The specimens were exposed to the targeted constant temperature and humidity (temperature of 85 °C and a relative humidity of 95%) for the predefined durations. The steam curing was carried out in different batches.

### ***Optimization of steam curing duration***

To get the optimum duration for SC that can satisfy all the requirements of UHPC, all UHPC mixtures (M0 to M5) were subjected to steam curing for different trial durations in the range of 2 to 10 hours. The specimens were tested for compressive strength after steam curing for different durations. An optimum duration for steam curing was selected based upon the achievement of a maximum compressive strength in a minimum duration of the steam curing.

The step-by-step procedure for selecting the optimum duration of steam curing is as follows:

- A total of 18 cube specimens of 50 mm size were cast using mixture M0 (six durations  $\times$  three replicate for each duration of steam curing).
- The specimens, after demolding, were subjected to different durations of steam curing (0, 2, 4, 6, 8 and 10 hours).
- After exposure to the steam curing, the specimens were taken out from the oven and left for half an hour to cool down before testing them to determine the compressive strength.
- Like reference UHPC mixture (M0), the same procedure was used for other five UHPC mixtures containing natural pozzolan as partial replacement of Portland cement and silica fume (M1 through M5).

### 3.8.3 Accelerated carbonation curing set up

A purpose-built ACC cylindrical chamber was fabricated, as shown in Figure 3.5. The cylindrical shape of the chamber was chosen to sustain the high pressure. The inside diameter and height of the chamber were 400 and 500 mm, respectively. To place the concrete specimens inside the chamber, 250 mm diameter hole was made at the top of the chamber with 350 mm cover plate. For ensuring the safety, the chamber was made of steel with a wall thickness of 8 mm. Two holes, one as inlet and another as outlet, were made through the wall. The inlet was connected to the CO<sub>2</sub> cylinder by a pipe and the outlet was connected to a pressure gauge to measure inside chamber pressure. To prevent corrosion of the steel wall, the wall was epoxy-coated. Figure 3.6 shows the set-up used for the ACC.



**Figure 3.5: Set-up for the ACC**

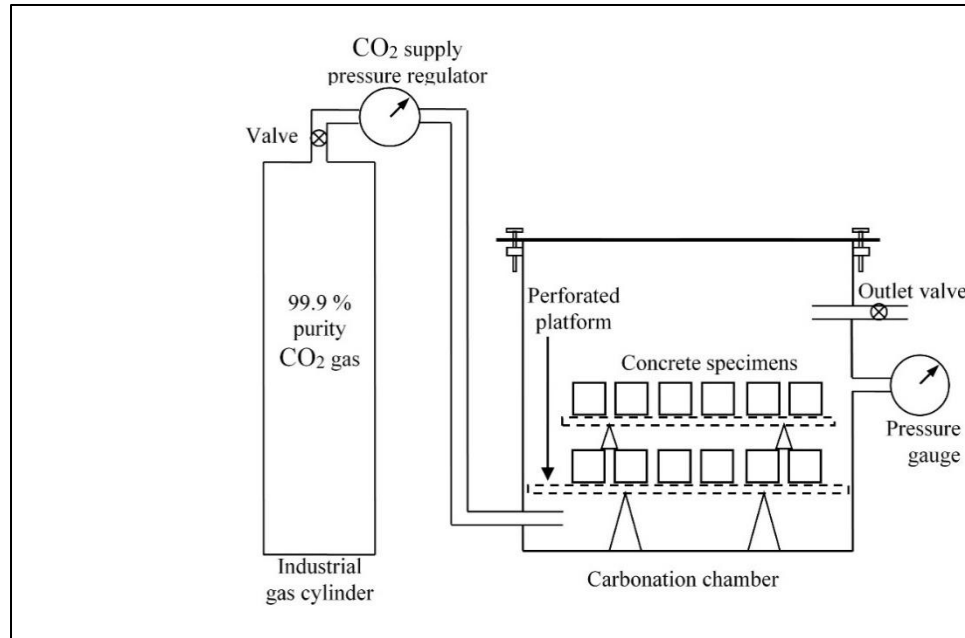


**Figure 3.6: Schematic diagram of ACC set-up**

The procedure for carrying out ACC is as follows:

- The valve of CO<sub>2</sub> cylinder was opened keeping the outlet valve of carbonation chamber opened for about 1 minute to flush out the air from the carbonation chamber so that the chamber will be almost fully filled by CO<sub>2</sub> gas. Then the outlet valve of the carbonation chamber was closed.
- The gas flow rate was regulated and stabilized in about 2 minutes, using the pressure gauge mounted on the chamber. This was done to maintain a constant intended pressure for ACC.
- After 10 hours of exposure at the intended pressure, the gas supply was closed, and the chamber was depressurized in order to retrieve the CO<sub>2</sub> cured batch.
- It is important to mention that one should carefully monitor the chamber at least for half an hour to ensure that there is no leakage and the pressure is stable.

### ***Optimization of CO<sub>2</sub> pressure for ACC***

Different combinations of four pressures (50, 60, 80 and 100 psi) with 10 hours exposure duration were chosen to carry out ACC for finding the optimum pressure to be used for ACC in the present study. Three cubes were used for each combination of pressure. A pure CO<sub>2</sub> gas was used (99.9% CO<sub>2</sub> concentration). After taking out the specimens from the ACC chamber and leaving them in air for 1 hour, they were tested in compression by applying load at a rate of 2 kN/s to obtain compressive strength.

### **3.9 Testing of Hardened UHPC Specimens**

All specimens used to test for obtaining hardened properties of the UHPC mixtures were demolded after six hours of casting. As mentioned earlier, the specimens were subjected to three curing regimes, i.e., burlap curing (BC), accelerated carbonation curing (ACC), and steam curing (SC) before conducting any test. The ACC was carried out using selected optimum pressure and duration (100 psi constant pressure for 10 hours). The steam curing was carried out for an optimum duration of 6 hours.

The mechanical tests conducted on the UHPC specimens included compressive strength, splitting tensile strength, modulus of elasticity, and fracture toughness tests. Drying shrinkage was monitored for four months. The chloride permeability was determined to indicate the durability. SEM was conducted to study the morphology of the specimens.

#### **3.9.1 Details of the tests for each curing regime**

Table 3.10 shows the details of UHPC specimens used for conducting various tests for each of the six mixtures and three curing regimes.

**Table 3.10: Details of specimens of various tests per mixture**

S/N	Test	Test Method	Specimen Dimensions	Test Age
1	Compressive strength	ASTM C 39	100 × 100 × 100 mm cube	7, 14 and 28 days
2	Modulus of elasticity	ASTM C 469	75 × 150 mm cylinder	28 days
3	Split tensile strength	ASTM C 496	75 × 150 mm cylinder	28 days
4	Fracture Toughness	ASTM E1290	40 × 40 × 160 mm prism specimens (notched at mid span)	28 days
5	Chloride permeability	ASTM C 1202	75 × 150 mm cylinder	28 days
6	Shrinkage	ASTM C 157	50 × 50 × 250 mm prism	Up to 4 months
7	Morphology of the microstructure	SEM	50 × 50 × 50 mm cube	28 days

The specimens required to conduct various tests were cast for each mixture and curing regime, that included specimens of various sizes and different shapes (cubes, cylinders, prisms, etc.) as shown in Figure 3.7. Three replicate specimens were used to obtain average values. Figure 3.7 shows the specimens prepared for conducting different tests for one of the six UHPC mixtures. As shown in Figure 3.7, mixture ID, specimen number and curing regime were written on each specimen.

The specimens were divided into three groups with the same number of specimens, each group has different curing regime (SC, ACC and BC). For SC, the specimens were taken inside an oven maintained at 85 °C temperature and 95% RH for a duration of six hours. For ACC, the specimens were placed inside the ACC chamber where they were exposed to carbon dioxide at a pressure of 100 psi for a duration of 10 hours. For BC, the specimens were covered with wet burlap sheets for a duration of 14 days.



**Figure 3.7: Preparing of the test specimens**

### 3.9.2 Compressive strength

The compressive strength was determined in accordance with ASTM C 39 for cubes. Cube specimens of 100 mm size were used to determine the compressive strength of all the mixtures after 7, 14, 28 and 90 days of air exposure following the curing regimes (ACC for 10 hours and SC for 6 hours) [45]. The specimens subjected to BC were tested for



compressive strength after 10 hours, 7 days and 14 days of burlap curing. Two sets of specimens were also tested after 28 and 90 days of air exposure after BC. The cubes were tested using a 3000 kN capacity automatic compression testing machine of hydraulic type (MATEST) as shown in Figure 3.8. Compressive load was applied at a rate of 5 kN/s. Figure 3.8 also shows the failure of the cubes after compression testing. Unlike normal concrete, the failure of UHPC occurred due to development of multiple vertical cracks due to the presence of fibers in UHPC.



**Figure 3.8: Compressive strength test preparation**

### **3.9.3 Modulus of elasticity**

ASTM C 469 standard test method was used for determining the static modulus of elasticity [46]. Cylindrical specimens of size  $75 \times 100$  mm were used to determine the elastic modulus for all the mixtures after 28-days of air exposure following the curing regimes. The specimens were tested using the same automatic testing machine used for compressive strength test (MATEST). The compressive loading rate was 2 kN/s. The load and the



corresponding deformation were recorded for each specimen using a data logger. Installation of test equipment and specimens after testing is shown in Figure 3.9.



**Figure 3.9: Modulus of elasticity test installation**

As shown in Figure 3.9, the specimen was clamped in two circular steel frames by three screws on each frame, two Linear Variable Differential Transformer (LVDTs) were placed vertically on opposite sides to consider any movement on specimen sides, one LVDT placed perpendicular to the movable plate of the compression machine to measure its movement. The linear deformations were captured by the LVDTs and the load was sensed

by the load cell, which was placed under the specimen. LVDTs and load cell were connected to a data logger.

The elastic portion of the compressive stress-strain curve up to 40 percent of the ultimate compressive strength ( $0.4 f_c'$ ) was used to determine the modulus of elasticity. The modulus of elasticity was calculated using the following formula:

$$E = \frac{S_2 - S_1}{\epsilon_2 - 0.000050}$$

Where:

$E$  = Modulus of elasticity, MPa,

$S_2$  = Stress corresponding to 40 % of ultimate load,

$S_1$  = Stress corresponding to a longitudinal strain,  $\epsilon_1$ , of 50 millionths, MPa, and

$\epsilon_2$  = Longitudinal strain produced by stress  $S_2$ .

It is worthy to note that the distance between the circular steel frames is 87 mm, which used to calculate the strain of the specimens.

### **3.9.4 Split tensile strength**

The split tensile strength test is an indirect test to measure the tensile strength of concrete using ASTM C 496 (Figure 3.10). Cylindrical specimens of 75 mm diameter and 150 mm high were used for split tensile strength test after air exposure of 28 days following the curing regimes. The same equipment used for compressive strength test were used for split tensile strength test as shown in Figure 3.10.



**Figure 3.10: Split tensile strength test installation**

The tensile strength was calculated using the following equation [34]:

$$f_t = \frac{2 P}{\pi l d}$$

Where:

$f_t$  = tensile strength, MPa

$P$  = load applied to the cylinder, N

$l$  = Length of the cylinder, mm

$d$  = diameter of the cylinder, mm

### 3.9.5 Drying shrinkage

Drying shrinkage is defined as the shrinkage of a hardened concrete element due to the loss of capillary water. This shrinkage induces tensile stress, which may lead to cracking, internal warping, and external deflection, of concrete [48]. The drying shrinkage test was conducted according to ASTM C 157 [49]. Three prism specimens of size  $50 \times 50 \times 250$  mm were used for measuring the drying shrinkage of the specimens belonging to each curing regime and each mixture. A data logger as shown in Figure 3.11 used to measure the change in length with time.

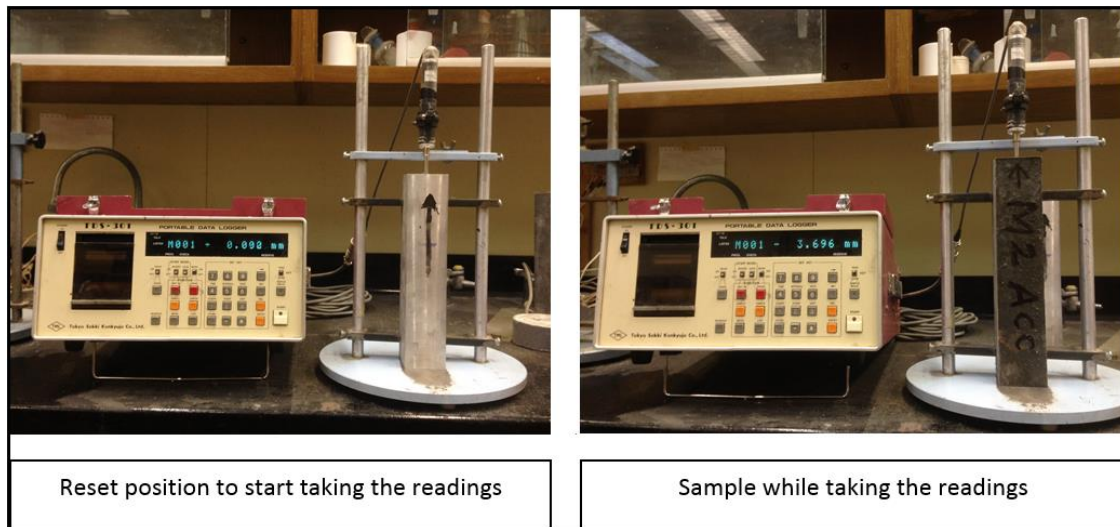


**Figure 3.11: Drying shrinkage apparatus and measurements**

The first reading was set as the initial reading considered as a reference for other readings. The first reading for all the specimens were taken after 1 day of curing to get a fixed duration for all curing regimes and all mixtures. After recording the change in length, strain was calculated from the following formula:

$$\text{Strain} = \frac{\text{change in length}}{\text{gauge length (250 mm)}}$$

### 3.9.6 Fracture toughness

It is reported that UHPC has excellent fracture properties besides its very high strength and elasticity due to the addition of fibers to UHPC. The addition of fibers makes it capable of resisting the fracture owing to its ductility [50]. The ductile behavior of UHPC specimens was tested through cyclic loading and unloading. The data collected through this test was used to study the fracture properties of different UHPC mixtures in terms of critical stress intensity factor ( $K_{ic}$ ).

Prism specimens with dimensions of 40×40×160 mm and with a central notch created at the bottom was used for the fracture toughness test. Fracture toughness test was conducted after 28 days of air exposure following three curing regimes (SC, ACC and BC).

Two-Parameter Fracture Model (TPFM) was used to determine the fracture properties. For TPFM: a span-to-depth ratio ( $S/d$ ) of 3; initial notch depth ( $a_0$ ) as one-third of the total depth of the beam (~13 mm), and the notch width of 4 mm were used. Three-point bending with the load ( $P$ ) and crack mouth opening displacement (CMOD) were measured for single edge notched beam specimen, as shown in Figure 3.12. TPFM was used to determine the critical stress intensity factor ( $K_{ic}$ ) and critical crack tip opening displacement ( $CTOD_c$ ) of a monolithic beam based on an effective elastic crack approach. The nonlinear fracture behavior was accounted for by using linear elastic fracture mechanics equations to calculate the effective elastic crack length based on the measured loading and unloading compliance of the beam. The geometric factors were included in the calculations to account for the geometry and size of the beams. INSTRON machine of 600 KN capacity as shown in Figure 3.13 was used to conduct this test.

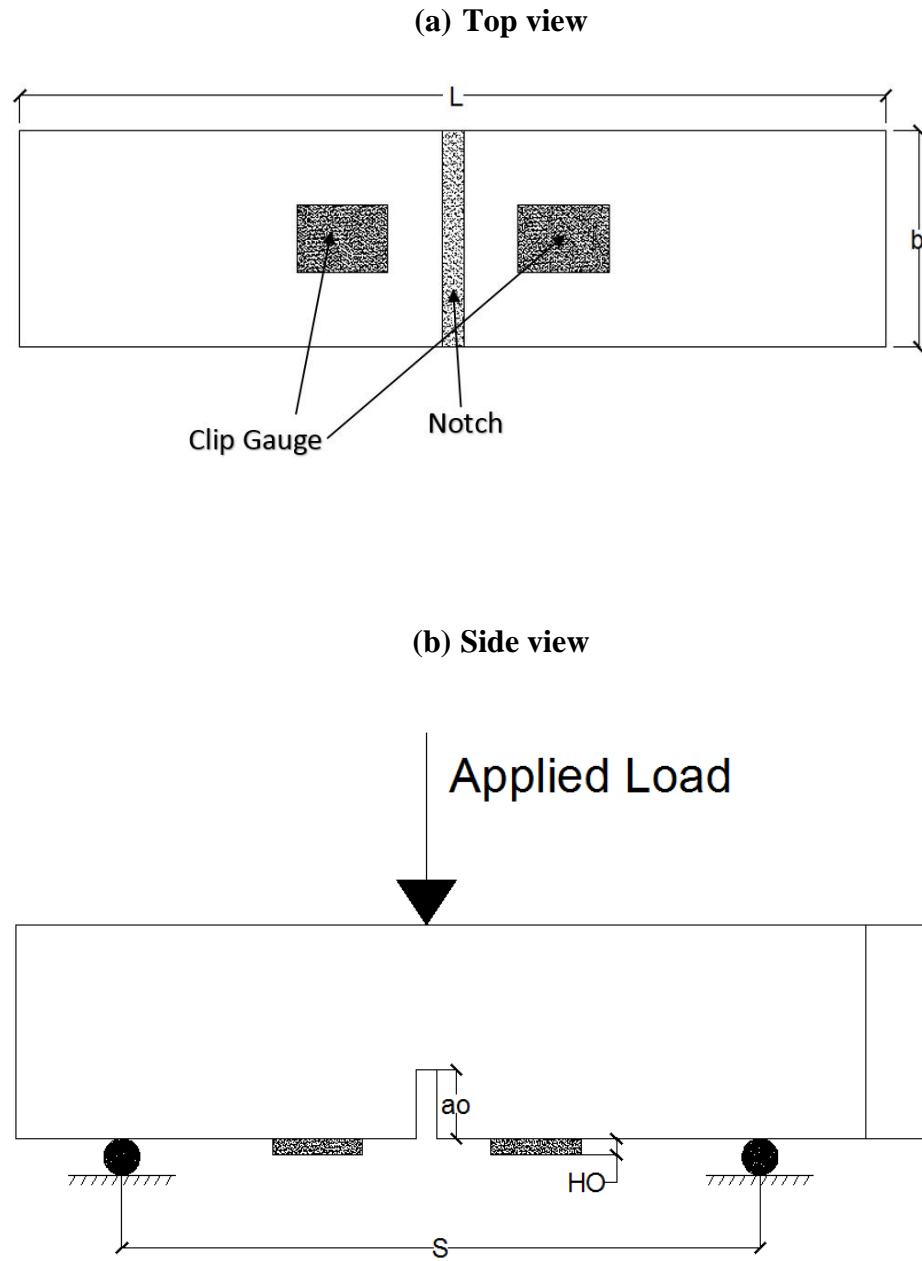


**Figure 3.12: Details of clip gauge attached to UHPC prisms used to measures the displacement of crack mouth opening (CMOD).**





**Figure 3.13: Complete test setup for measuring fracture toughness test.**

The two fracture parameters were determined using the TPFM are the  $K_{Ic}$  and  $CTOD_c$ . These were computed by first obtaining the critical effective crack length ( $a_c$ ). By equating, the concrete's modulus of elasticity from the loading and unloading curves ( $E = E = E_u$ ) as shown in equations below, the critical effective crack length ( $a_c$ ) could be determined as follows:

$$E_i = \frac{6Sa_0g_2(\alpha_0)}{C_id^2b}$$

$$E_u = \frac{6Sa_cg_2(\alpha_c)}{C_id^2b}$$

While:

$$\alpha_0 = \frac{(a_0 + HO)}{(D + HO)}$$

$$\alpha_c = \frac{(a_c + HO)}{(D + HO)}$$

$$g_2(\alpha) = 0.76 - 2.28\alpha + 3.87\alpha^2 - 2.04\alpha^3 + \frac{0.66}{(1 - \alpha)^2}$$

Where:

$S$  = the span length.

$d$  = the span depth

$b$  = the span width.

$a_0$  = the initial notch depth of the beam

$\alpha_0$  = the initial notch/depth ratio

$\alpha_c$  = the critical notch/depth ratio

$HO$  = the thickness of the clip gauge holder.

$g_2(\alpha)$  is the opening displacement geometric factor for the Three-Point Bending (TPB).

Once the  $a_c$  is computed, then the critical stress intensity factor ( $K_{ic}$ ) could be calculated from the following:

$$K_{ic} = 3\left(P_c + \frac{0.5W_0S}{L}\right) + \frac{S\sqrt{\pi a_c}g_1\left(\frac{a_c}{d}\right)}{2d^2b}$$

Where:

$P_c$  = the peak load.

$W_0$  = the weight of the specimen.



$L$  = the length of the specimen.

$g_1$  is the stress intensity factor geometric function for the beam specimen calculated from the following equation:

$$g_1\left(\frac{a_c}{d}\right) = \frac{1.99 - \left(\frac{a_c}{d}\right)\left(1 - \frac{a_c}{d}\right)[2.15 - 3.93\left(\frac{a_c}{d}\right) + 2.70\left(\frac{a_c}{d^2}\right)]}{\sqrt{\pi}\left[1 + 2\left(\frac{a_c}{d}\right)\right]\left[1 - \left(\frac{a_c}{d}\right)\right]^{2/3}}$$

Then, we can find the  $CTOD_c$  using the following equation:

$$CTOD_c = 6\left(P_c + \frac{0.5W_0S}{L}\right) \times \frac{Sa_c g_2\left(\frac{a_c}{d}\right)}{Ed^2b} \\ \times [((1 - (a_c/a_0))^2 + [1.081 - 1.149\left(\frac{a_c}{d}\right)] \times \left[\left(\frac{a_c}{a_0}\right) - \left(\frac{a_c}{a_0}\right)^2\right])^{1/2}]$$

Where:

$$g_2\left(\frac{a_c}{d}\right) = 0.76 - 2.28\left(\frac{a_c}{d}\right) + 3.87\left(\frac{a_c}{d}\right)^2 - 2.04\left(\frac{a_c}{d}\right)^3 + \frac{0.66}{(1 - a_c/d)^2}$$

Where:

$C_i$  = The loading compliance, which was calculated as the inverse of the slope start from 10% until 50% of the peak load. This should have estimated to be in the linear elastic range without any initial seating load discontinuities in the curve.

$C_u$  = The unloading compliance, which is the inverse of slope of the unloading curve. it should be calculated in the range of 10% and 80% of the peak load on the unloading curve.

Bordelon described the criteria of  $C_i$  and  $C_u$  determination as shown in Figure 3.14 [51].

Figure 3.15 shows the fracture toughness test set-up and failure of some specimens.

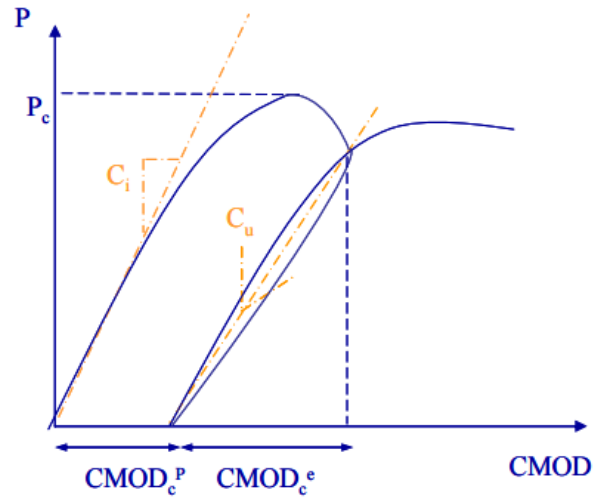


**Figure 3.14: Loading and unloading compliance  $C_i$  and  $C_u$ .**

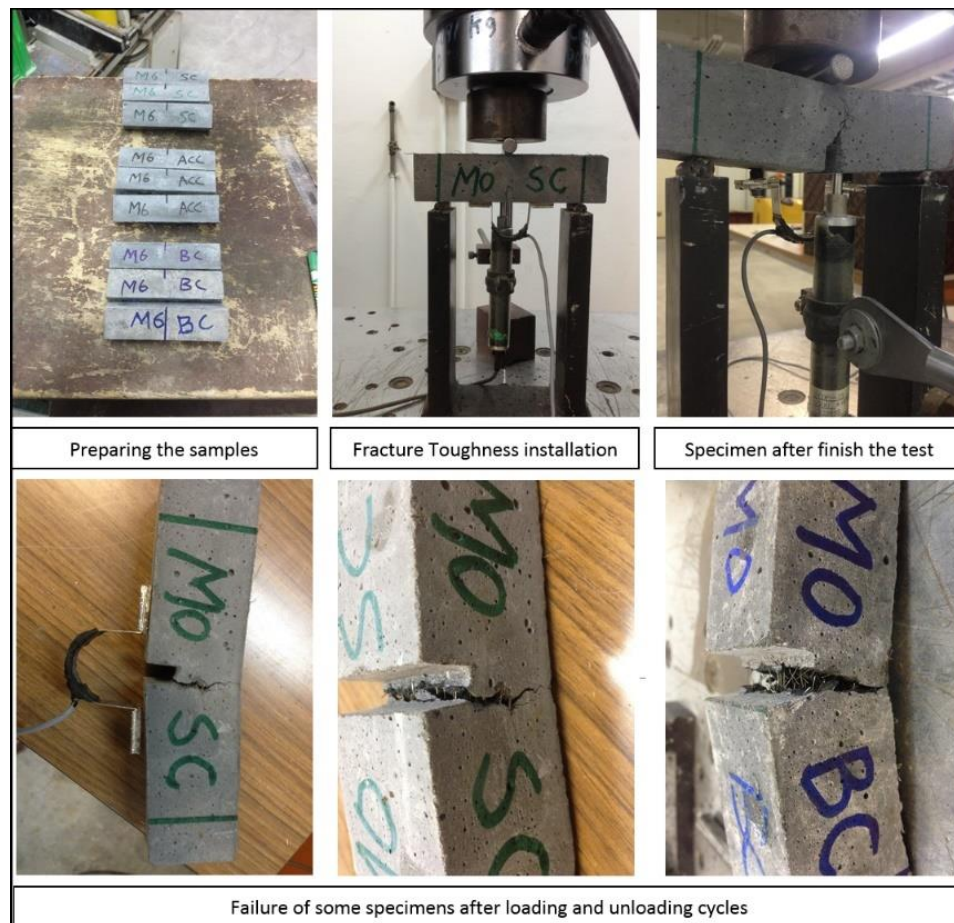


**Figure 3.15: Fracture toughness specimen's preparation, installation and testing**

### 3.9.7 Chloride permeability

The chloride permeability test is a rapid test performed to determine the electrical resistance of concrete against the penetration of chloride. This test is conducted according to the standard method given in ASTM C 1202 [52]. The test was conducted by using PROOVE IT instrument (Germann Instruments) as shown in Figure 3.16.

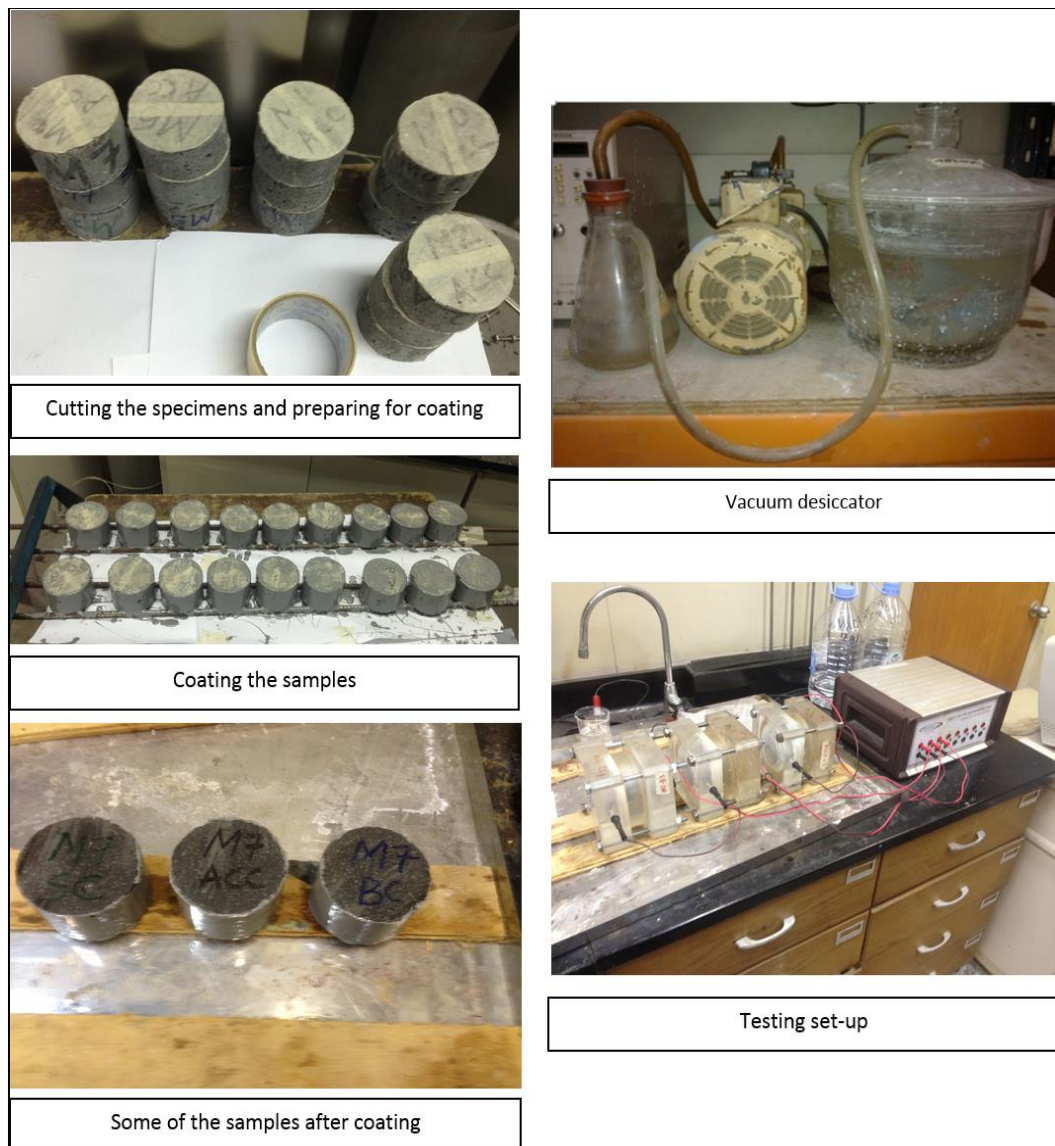


**Figure 3.16: Chloride permeability test machine and sample preparation**

The procedure adopted for this test is as follows:

- A 50 mm thick concrete disk was cut out from the middle of the  $75 \times 150$  mm cylindrical specimens.
- The curved surface of the cylinder was coated with an epoxy to prevent evaporation of moisture.
- Before testing, the disks were conditioned in vacuum desiccator, then they were saturated with water and kept for 24 hours.
- After that, rubber gaskets were fixed around the specimens to fix it. Then the specimens were placed in between the plexiglass measuring cells.
- Water leakage test should be conducted before adding the solutions in the cells.
- 3% NaCl solution was filled into the black head half-cell while the other half was filled with 0.3 N NaOH solution.
- A potential difference of 60 Volt DC was maintained across each cell holding the specimens and the total charge passed in coulombs was recorded at the end of the test, which continues for 6 hours.

### **3.9.8 Scanning electron microscopy (SEM)**

Scanning electron microscopy (SEM) is one of the most advanced technical tools that can be used to study and analyze concrete microstructure. The high resolution achieved by using SEM, which reaches to about 2.5 nm, makes this test useful. In addition, SEM test can be used to find the elemental composition of the material tested [53]. In this study, different samples distributed all over the mixtures were tested. Small portions were taken from the crushed specimens, and then these specimens were kept in a plastic bag, and

placed inside a desiccator until testing. The sample preparation and the set-up of the SEM used in this research are shown in Figure 3.17.



**Figure 3.17: Scanning electron microscope**

## CHAPTER 4

### RESULTS AND DISCUSSIONS

In this chapter, results and discussion pertaining to the evaluation of performance of the different UHPC mixtures subjected to different curing regimes are presented. The results of compressive strength, modulus of elasticity, split tensile strength, fracture toughness, drying shrinkage, chloride permeability, and scanning electron microscopy were compiled in tabular and figure forms and important conclusions were drawn based on the logics and comparison of the results of the present study with those published in literature.

#### 4.1 Selection of Optimal Duration of Steam Curing (SC)

The compressive strength of the all the mixtures was measured with and without SC for different durations. Table 4.1 shows the compressive strength values for all the mixtures with and without SC for 2, 4, 6, 8 and 10 hours. From Table 4.1, a significant improvement in compressive strength of all mixtures due to steam curing can be observed.

**Table 4.1: Compressive strength values with and without SC**

SC duration (Hours)	Compressive strength (MPa)					
	M0	M1	M2	M3	M4	M5
0	70.1	68.0	63.6	65.4	60.8	52.3
2	103.7	101.4	100.3	102.6	97.4	91.7
4	120.4	117.6	114.8	118.3	114.1	105.6
6	142.7	136.8	134.2	139.5	133.7	127.2
8	153.1	147.0	144.3	150.8	142.8	136.0
10	162.8	155.3	154.9	158.3	151.7	144.6

The plots of compressive strength of the mixtures without and with SC, as shown in Figures 4.1 and 4.2 indicate a clear increase in the compressive strength due to exposure to SC. The increase in compressive strength with the duration of SC is sharper at early stage, for example, an improvement in the compressive strength as high as 75% is noted when the mixture M5 was subjected to SC for first two hours. The rate of increase in strength at higher durations of SC was slowed down, particularly after six hours of the SC. It can be noted from the data in Figure 4.2 that, for example, the compressive strength of mixture M5 was increased by 20% when the curing duration was increased from 4 to 6 hours, However, an increase of strength of mixture M5 by only 7% was observed when the curing duration was increased from 6 to 8 hours. Therefore, considering the strength and energy saving, SC for a duration of 6 hours was considered as optimum for all the UHPC mixtures.

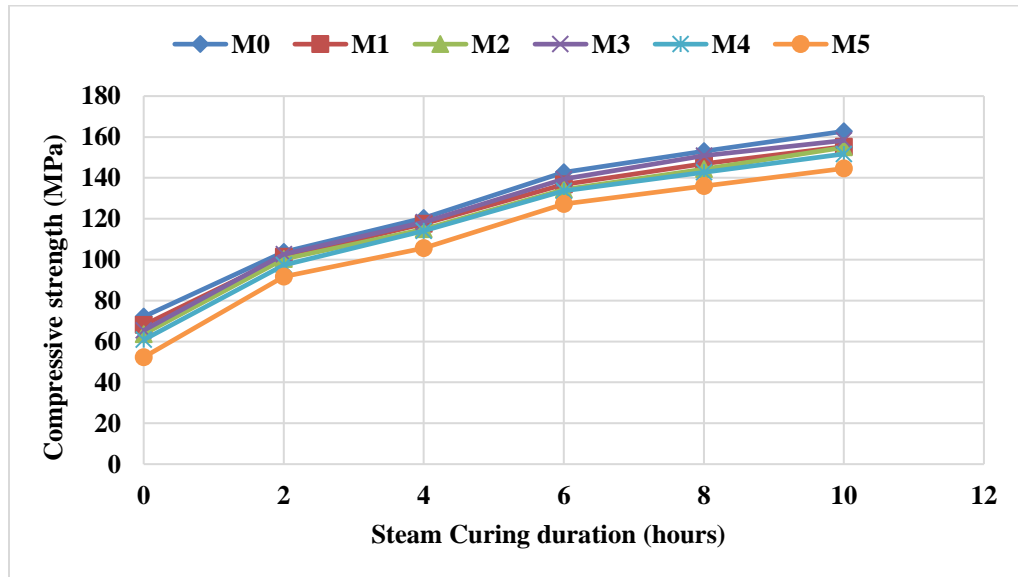


**Figure 4.1: Compressive strength of UHPC mixtures under SC**

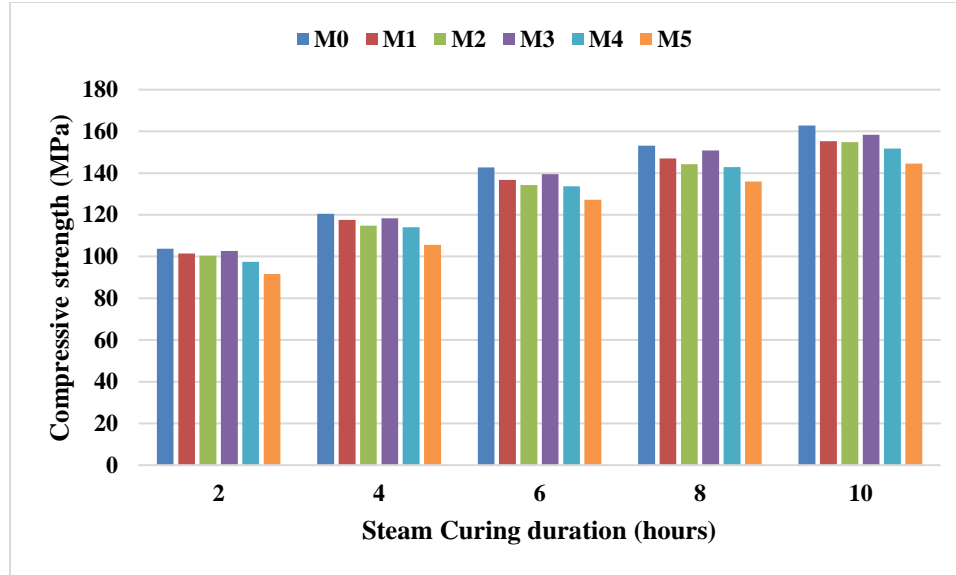


**Figure 4.2: Compressive strength values at different SC periods**

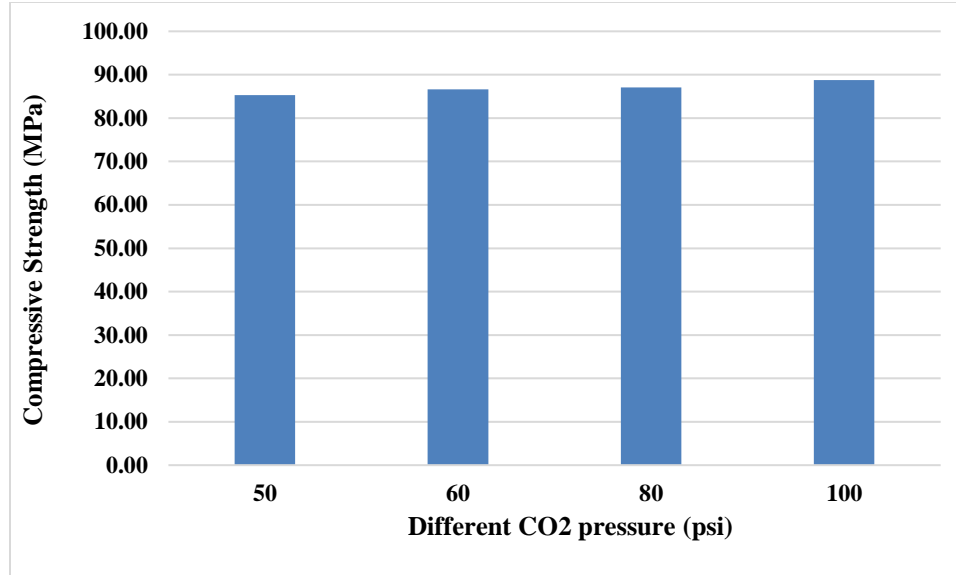
## 4.2 Selection of Optimal Pressure of Accelerated Carbonation Curing (ACC)

Table 4.2 shows the compressive strength of the UHPC mixture M0 after 10 hours of ACC at different pressures. Compared to the compressive strength of 79 MPa for the mixture M0 without ACC, the strength of the same mixture increased significantly after exposure to ACC. However, the increase in pressure of ACC did not affect the compressive strength significantly, as evident from the data in Figure 4.3. In the present work, a pressure of 100 psi was considered as an optimum pressure for carrying out ACC of all mixtures for 10 h.

**Table 4.2: Compressive strength of M0 after 10 h of ACC at different pressures**

CO <sub>2</sub> pressure (psi)	Compressive strength (MPa)
50	85
60	87
80	87
100	89





**Figure 4.3: Compressive strength at different CO<sub>2</sub> pressures**

Table 4.3 summarizes the optimum conditions adopted for each of three curing regimes used for all UHPC mixtures:

**Table 4.3: Summarization of curing regime properties**

Curing Regime	Time before start curing (Hours)	Curing Duration	Curing specifications
SC	6	6 hours	85°C with 95% RH
ACC	6	10 hours	100 psi of CO <sub>2</sub>
BC	6	14 days	Burlap sheets

### 4.3 Workability

The flow test results of all six UHPC mixtures obtained in accordance with ASTM C 1437 are plotted in Figures 4.4 and 4.5. All the UHPC mixtures satisfied the workability requirements as their flow values were in the range of targeted flow (180 to 220 mm). However, the addition of natural pozzolan as a partial replacement of silica fume or

Portland cement significantly reduced the workability. The decrease in workability due to an increase in the natural pozzolan may be attributed to the rough surface texture of the particles of natural pozzolan compared to that of the particles of Portland cement and silica fume.

The maximum limit for replacements of silica fume and Portland cement by natural pozzolan were kept as 50% and 30%, respectively. This was decided considering the fact that the addition of natural pozzolan beyond these limits would decrease the flow below minimum value of 180 mm, as can be seen from Figures 4.4 and 4.5, unless the dosage of superplasticizer is increased which may cost more than saving due to an increase in the dosage of natural pozzolan.

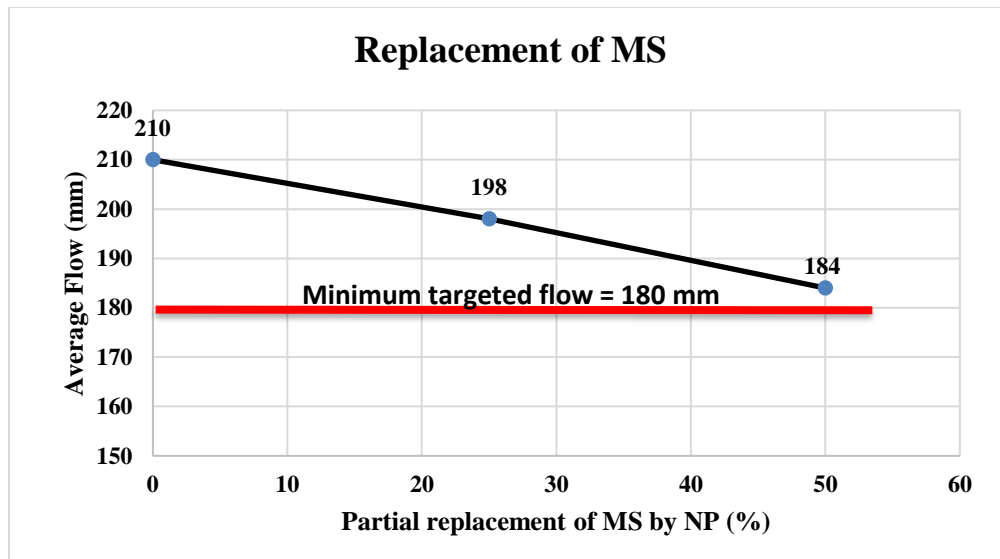


**Figure 4.4: Decrease in flow with increase in level of replacement of MS by NP**

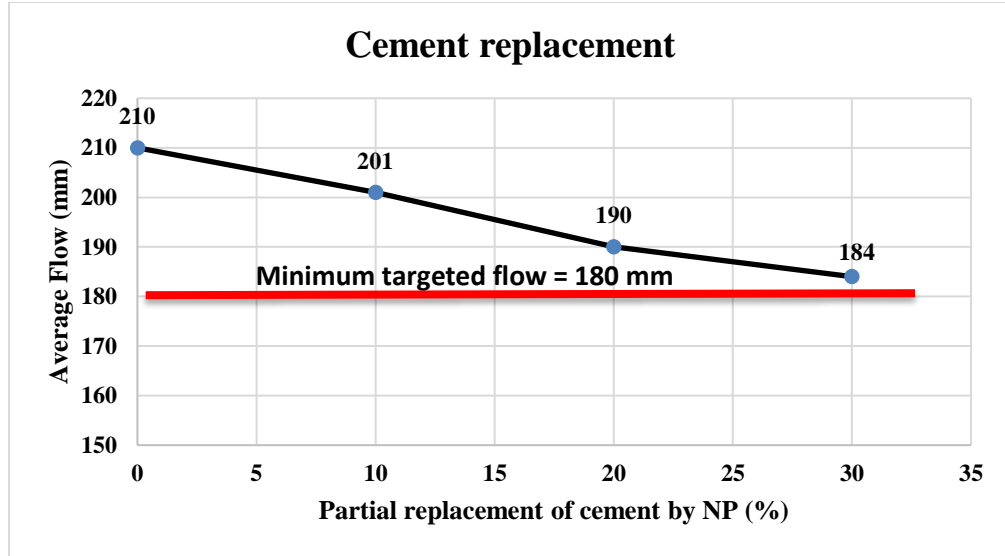


**Figure 4.5: Decrease in flow with increase in level of replacement of cement by NP**

#### **4.4 Compressive Strength**

Specimens belonging to all three curing regimes were tested for compressive strength at five different stages as follows:

- Directly after 6 hours of SC and after 7, 14, 28 and 90 days of exposure to air in laboratory conditions following the 6 hours of SC
- Directly after 10 hours of ACC and after 7, 14, 28 and 90 days of exposure to air in laboratory conditions following the 10 hours of ACC
- After 10 hours, 7 and 14 days of burlap curing and after 28, 90 days of exposure to air in lab conditions following the 14 days of BC

As mentioned earlier, all the specimens were demolded after six hours of casting and then they were exposed to the respective curing regimes.

The compressive strength test results of the six UHPC mixtures with three types of curing regimes are presented in Tables 4.4 through 4.6. The reported values of compressive strength are averages of three specimens prepared from each mixture for each curing method.

From the data in Table 4.4, it can be observed that all the UHPC mixtures subjected to SC attained a compressive strength of more than 150 MPa after exposure to air for 7 days after 6 hours of SC. However, the same UHPC mixtures subjected to ACC and BC attained a compressive strength of more than 150 MPa when exposure to air for 90 days after 10 hours of ACC and 14 days of BC, as can be seen from the data in Tables 4.5 and 4.6. Since air exposure does not need any resources and the UHPC mixtures cured using ACC and BC for 10 hours and 14 days, respectively, had strength more than needed for handling, transporting and installing the precast structural members, attaining strength of more than 150 MPa after 90 days in air is not an issue.

**Table 4.4: Compressive strength results for all SC specimens.**

Mixture ID	Compressive Strength (MPa)				
	Directly after SC	Air exposure (days) after SC			
		7	14	28	90
<b>M0-SC</b>	142.7	163.2	167.1	172.1	177.8
<b>M1-SC</b>	136.8	151.2	154.9	157.0	163.4
<b>M2-SC</b>	134.2	147.2	150.2	154.3	158.8
<b>M3-SC</b>	139.5	155.0	158.6	163.5	168.0
<b>M4-SC</b>	133.7	155.1	158.2	160.1	165.3
<b>M5-SC</b>	127.2	154.0	158.1	160.2	165.0

**Table 4.5: Compressive strength results for all ACC specimens.**

Mixture ID	Compressive Strength (MPa)				
	Directly after ACC	Air exposure (days) after ACC			
		7	14	28	90
<b>M0-ACC</b>	64.1	126.1	132.2	138.8	159.4
<b>M1-ACC</b>	61.7	122.8	129.9	137.5	154.2
<b>M2-ACC</b>	60.9	122.3	129.7	137.2	153.3
<b>M3-ACC</b>	61.4	121.4	130.2	135.6	155.0
<b>M4-ACC</b>	61.1	121.0	128.7	130.6	153.5
<b>M5-ACC</b>	60.1	118.4	128.2	130.6	152.0

**Table 4.6: Compressive strength results for all BC specimens.**

Mixture ID	(10 h BC)	Compressive Strength (MPa)			
		Testing age (days)			
		7 d BC	14 d BC	28 d in air	90 d in air
<b>M0-BC</b>	53.0	124.1	132.9	143.0	161.6
<b>M1-BC</b>	37.3	115.5	123.0	138.8	154.8
<b>M2-BC</b>	29.4	113.5	122.0	138.2	152.4
<b>M3-BC</b>	39.5	116.0	125.3	140.4	157.2
<b>M4-BC</b>	34.3	116.5	125.1	132.2	153.7
<b>M5-BC</b>	21.2	110.0	124.5	130.6	151.0

For all curing regimes, the strength of reference mixture M0 was found to be the highest compared to the mixtures with partial replacement of Portland cement and silica fume by natural pozzolan (M1 through M5). However, the difference between the strength of mixtures M1 through M5 and reference mixture M0 (kept in air for 90 days) is very low, around 8, 4 and 5% in cases of SC, ACC and BC, respectively. The difference between the strength of mixtures M1 through M5 is also very low for all the curing regimes. This indicates that the effect of partial replacement of Portland cement and silica fume by natural

pozzolan on compressive strength is not that significant as the effect of curing regimes and the duration of exposure to the air. Since natural pozzolan replacing Portland cement and silica fume has an insignificant adverse effect on compressive strength, all five mixtures (M1 through M5) can be adopted for the production of UHPC with economy and environmental benefits.

In order to highlight the effect of curing regimes on the evolution of compressive strength of UHPC mixture M0, the compressive strength versus time curves for different curing regimes (SC, ACC, and BC) are shown in Figure 4.6.

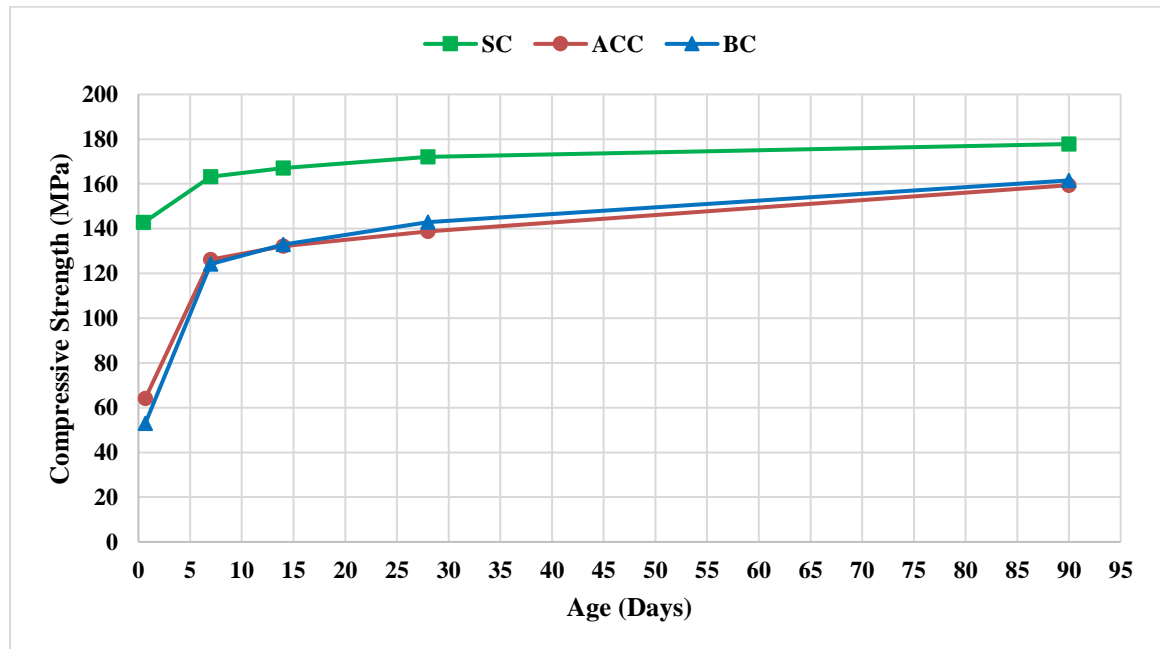


**Figure 4.6: Compressive strength of UHPC mixture M0 subjected to different curing regimes**

The data in Figure 4.6 indicate that the mixture M0 subjected to SC exhibited the highest compressive strength values at all stages. This is because the elevated temperature in SC regime accelerates the hydration process of UHPC specimens and the moisture due to water vapor compensate the loss in water due to high temperature, leading to a very high strength.

On the other hand, a lower heat of hydration in both ACC and BC resulting in a lower early strength than SC. Although the strength of mixture M0 subjected to ACC for 10 hours was slightly higher than that subjected to BC for 10 hours, the evolution of compressive strength of mixture M0 subjected to ACC and BC followed almost a similar path indicating that both curing regimes can be alternatively used.

An increase in the compressive strength by 14% was observed when specimens were exposed to air for 7 days after SC was applied. At later stages of air exposure, the compressive strength was increased at slow rate. The total increase in strength of mixture M0 exposed to air after SC for 6 hours was about 25%.

The compressive strength of specimens, exposed to air for 7 days after 10 hours of ACC, increased sharply by 97% and at later stage the increase in strength was at slow rate. The increase in strength of mixture M0 when exposed to air for 90 days after ACC for 10 hours was about 150%. A very high gain of strength during air exposure after 10 hours of ACC can be attributed to the fact that the carbonation on the surface of the specimens subjected to ACC results into the formation of an impervious layer that significantly reduces the evaporation of moisture from the core of the specimens. Due to prevention of the loss of water against evaporation, the hydration in ACC specimens continues for a long time increasing the strength heavily after the ACC treatment.

A sharp increase in the compressive strength of mixture M0 by 134% was noted when the duration of burlap curing was increased from 10 hours to 7 days. However, the increase in the compressive strength was only 7% when the duration of BC was increased from 7 days to 14 days. A further increase in the compressive strength by about 22% was observed when the mixture M0 was exposed to air for next 76 days after 14 days of BC. This

indicates that the BC for first 7 days followed by exposure to air would be sufficient to gain the intended compressive strength.

The plots showing evolution of compressive strength of the UHPC mixtures M1 through M5 subjected to three curing regimes (SC, ACC, and BC) are shown in Figures 4.7 through 4.11. It can be observed from Figures 4.7 through 4.11 that the trend of evolution of strength for all curing regimes to which the mixtures M1 through M5 were subjected to is almost similar to that of the reference mixture M0. This indicates that mixture composition has no significant impact on the trend of strength evolution under each of three curing regimes. However, there is a slight effect of the mixture composition on compressive strength for a given curing type and curing stage.

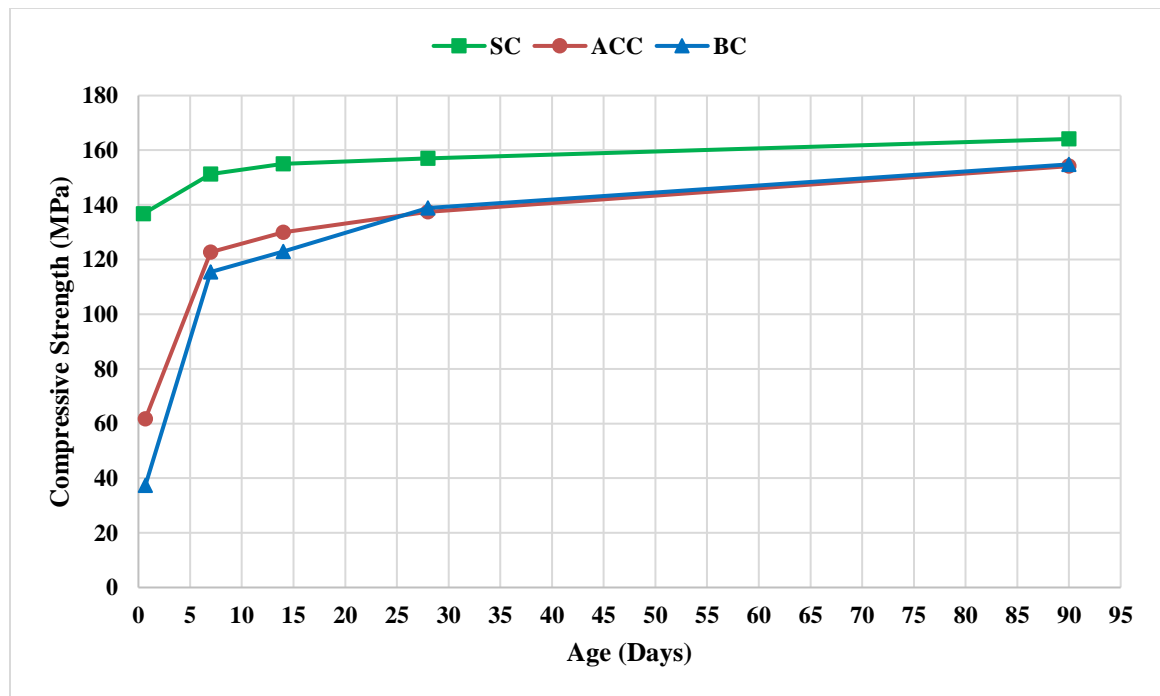


**Figure 4.7: Compressive strength of UHPC mixture M1 subjected to different curing regimes**



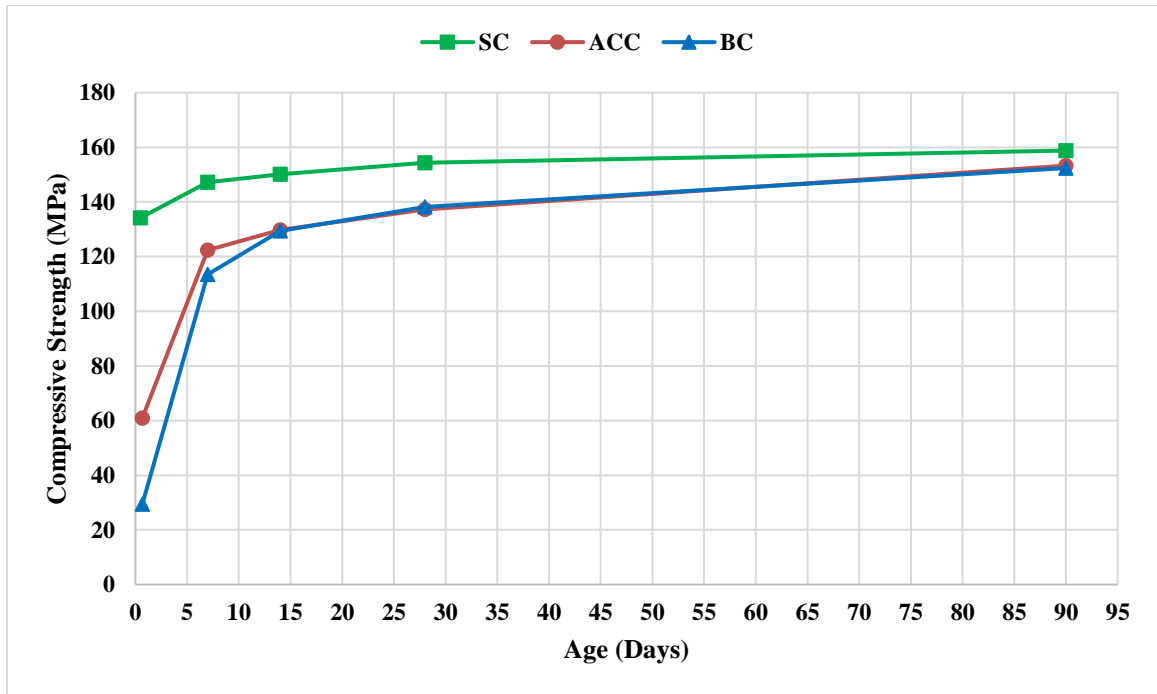


**Figure 4.8: Compressive strength of UHPC mixture M2 subjected to different curing regimes**

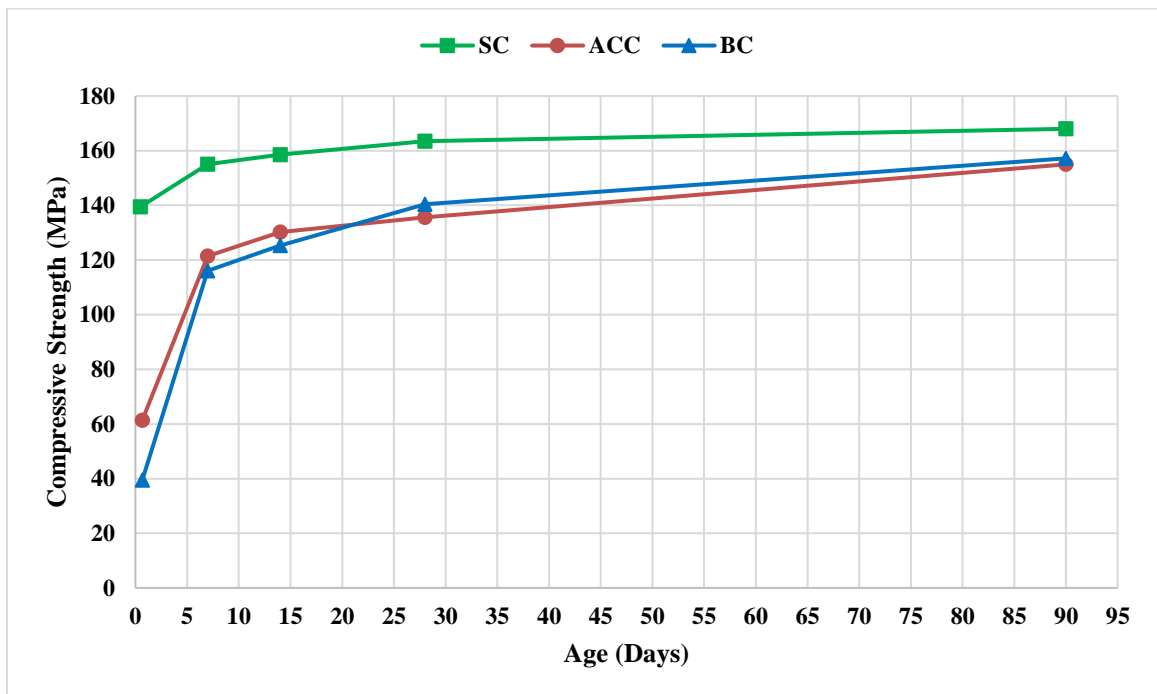


**Figure 4.9: Compressive strength of UHPC mixture M3 subjected to different curing regimes**

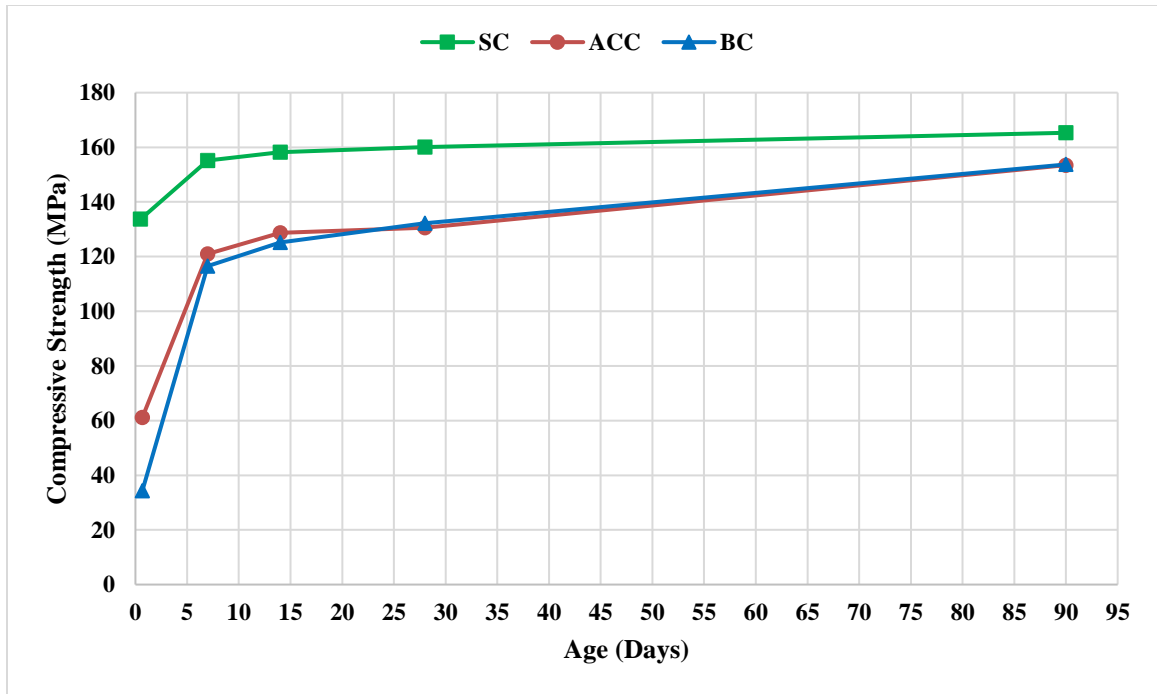


**Figure 4.10: Compressive strength of UHPC mixture M4 subjected to different curing regimes**

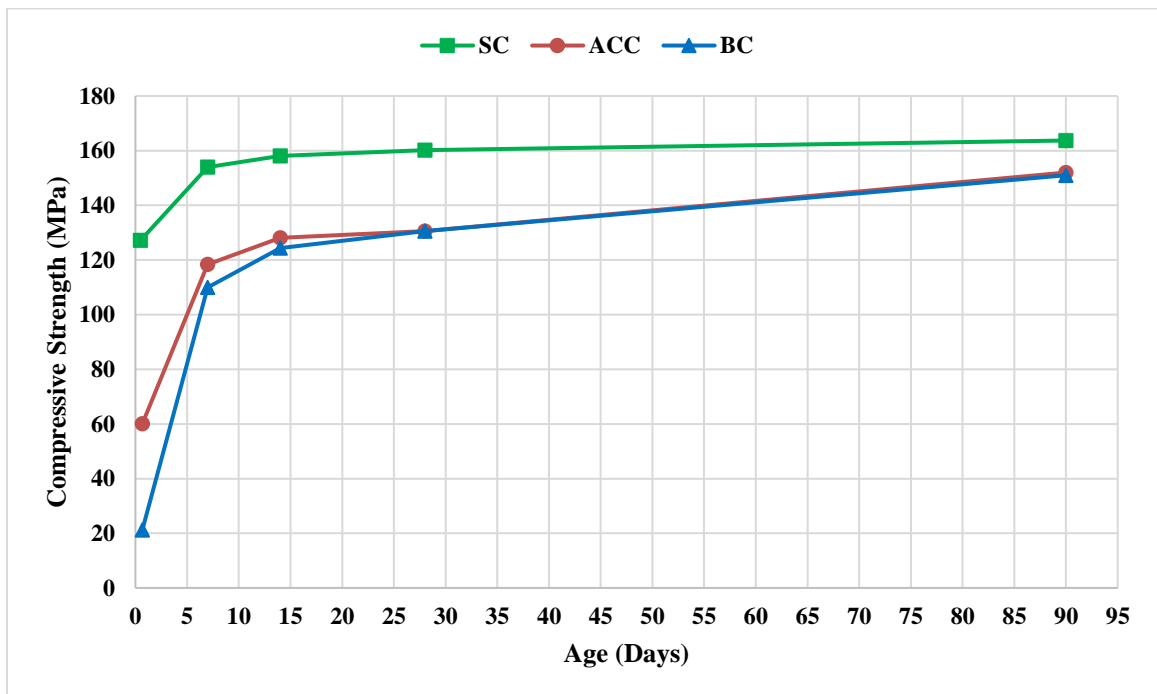


**Figure 4.11: Compressive strength of UHPC mixture M5 subjected to different curing regimes**

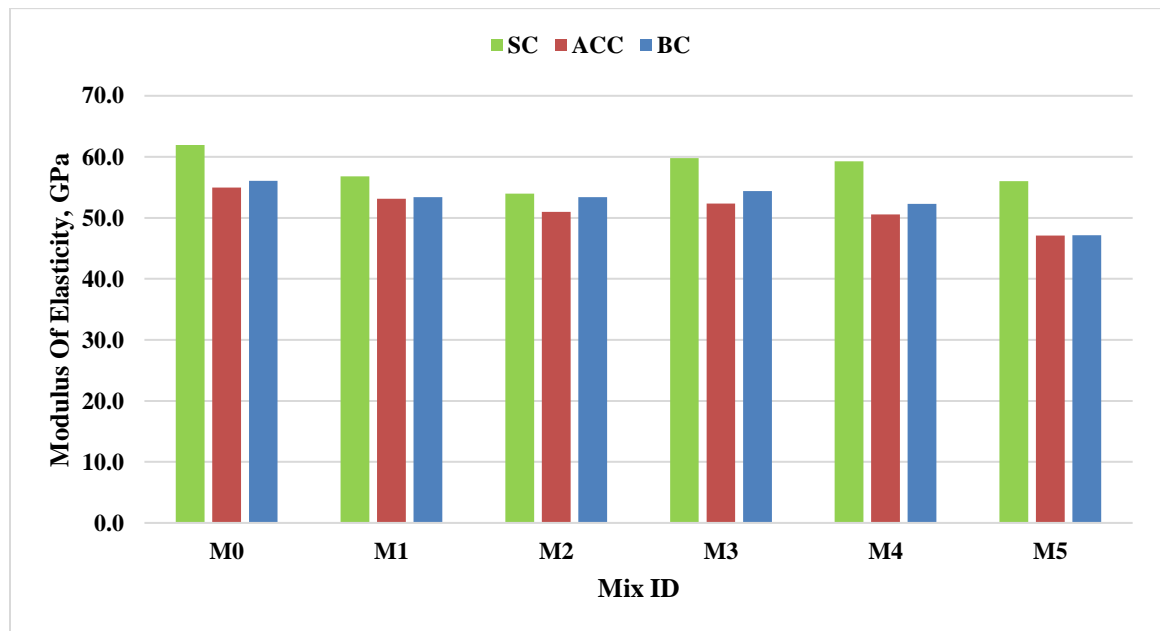
## 4.5 Modulus of Elasticity

Table 4.7 shows the modulus of elasticity of all the six UHPC mixture subjected to three types of curing and then exposed to air for 28 days.

**Table 4.7: Modulus of elasticity for all UHPC mixtures**

Curing Regime	Modulus of Elasticity (GPa)					
	Mixture ID					
	M0	M1	M2	M3	M4	M5
SC (6 h SC and 28 d air)	62	57	54	60	59	56
ACC (10 h ACC and 28 d air)	55	53	51	52	51	47
BC (14 d BC and 14 d air)	56	53	53	54	52	47

Similar to compressive strength, the highest values of the modulus of elasticity of mixtures were for SC regime, as shown in Figure 4.12. The reason for this improvement in the modulus of elasticity is the acceleration of hydration process at significant rate because of elevated temperature applied in SC.



**Figure 4.12: Modulus of elasticity of all UHPC mixtures**

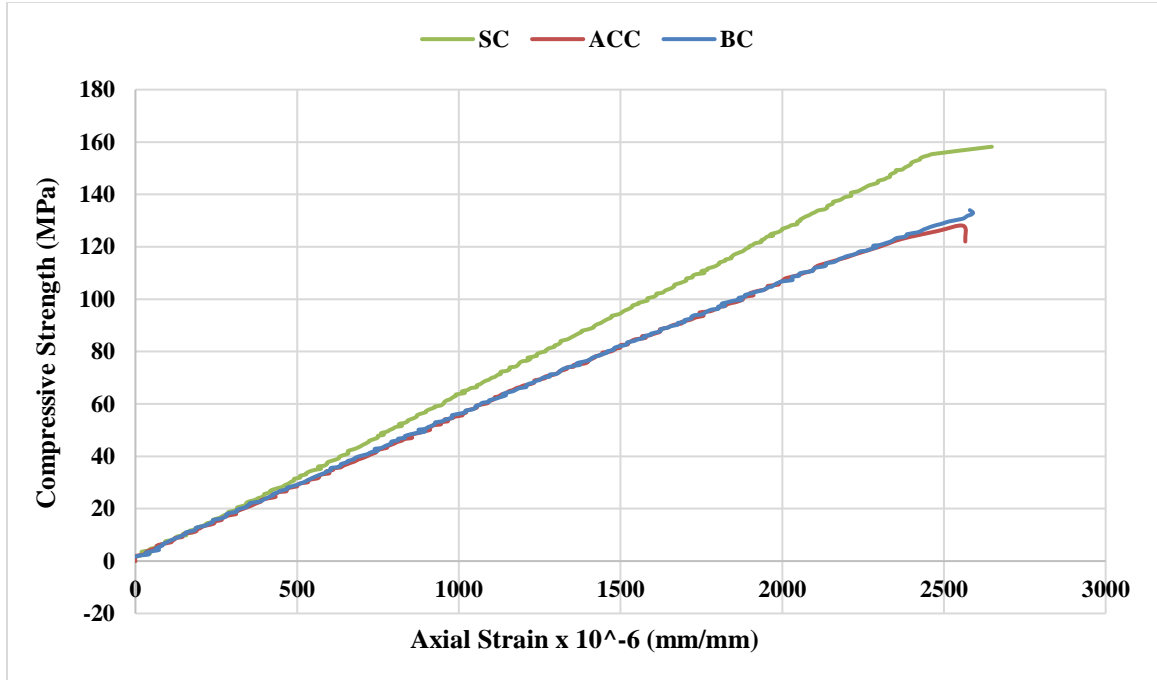


**Figure 4.13: Stress-Strain responses for M0 with different curing regimes**

The data in Figure 4.12 indicate that ACC and BC specimens have almost similar elastic modulus for all six mixtures. This is also confirmed by the same slope of the initial straight-line portion of the stress-strain curves for mixture M0 subjected to ACC and BC, as shown in Figure 4.13.

It may further be noted that unlike compressive strength that was significantly affected only by curing regimes, the modulus of elasticity is significantly affected by the composition of mixtures besides the curing regimes.

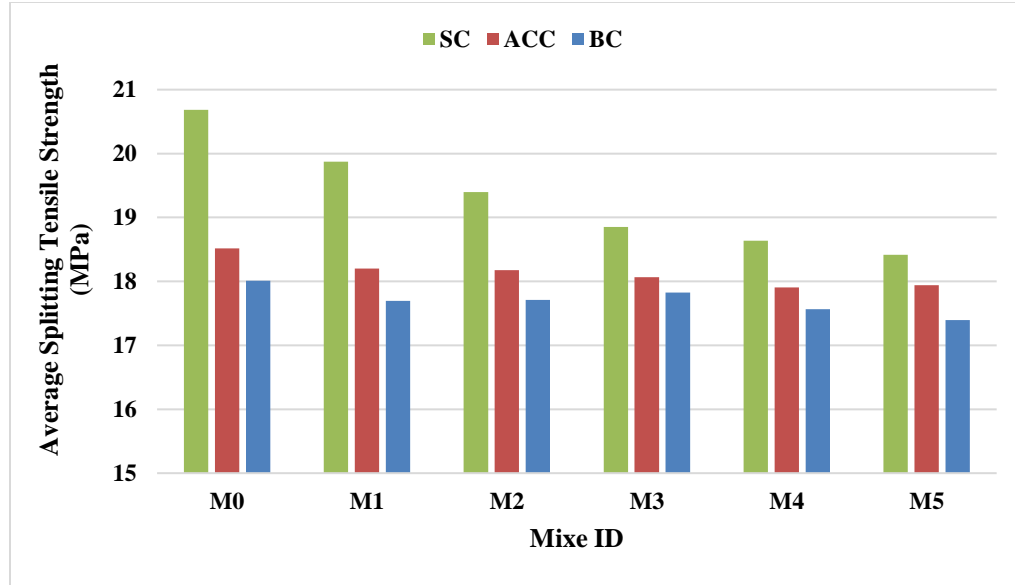
## 4.6 Splitting Tensile Strength

Table 4.8 shows the splitting tensile strength of all six UHPC mixtures subjected to three types of curing and then exposed to air for 28 days.

The data in Figure 4.14 show that the splitting tensile strength of the specimens subjected to SC is the highest for all the mixtures, followed by the splitting tensile strength values corresponding to ACC and BC. For example, mixture M0 subjected to SC had the splitting tensile strength 12% and 15% more than what it had when subjected to ACC and BC, respectively. The reason behind the higher splitting tensile strength values of SC related to the effect of steam treatment (high temperature and humidity) which accelerate the hydration process of the specimens. However, the data in Figure 4.14 clearly shows that this improvement decreases in the last mixture with only 2% improvement in SC specimens than ACC specimens and it is about 5% more than that in the BC specimens. This indicates that the splitting tensile strength is affected by curing regimes as well as by the composition of the mixtures. The reason behind a slightly increased splitting tensile strength of specimens subjected to ACC compared to those subjected to BC may be attributed to the fact that the formation of carbonation layer on the surface leads to a higher tensile strength of concrete.

**Table 4.8: Splitting tensile strength for all UHPC mixtures.**

Curing Regime	Splitting strength at 28 days (MPa)					
	M0	M1	M2	M3	M4	M5
SC (6 h SC and 28 d air)	20.7	19.9	19.4	18.9	18.6	18.4
ACC (10 h ACC and 28 d air)	18.5	18.2	18.2	18.1	17.9	17.9
BC (14 d BC and 14 d air)	18.0	17.7	17.7	17.8	17.6	17.4



**Figure 4.14: Splitting tensile strength for all UHPC mixtures**

## 4.7 Fracture Toughness

For each mixture, the readings of loading and unloading values were taken to find different parameters, which were used to determine the critical stress intensity ( $K_{ic}$ ) and critical crack tip opening displacement ( $CTOD_c$ ) factors for each mixture and each type of curing. Table 4.9 summarize the average fracture toughness results for all mixtures for the three curing regimes SC, ACC and BC.

The data in Figure 4.15 show that the values of  $K_{ic}$  for all six mixtures subjected to SC regime were the highest compared to ACC and BC curing regimes. This is in line with other mechanical properties, which were found to be the best in case of SC due to the positive effect of temperature and humidity in making the microstructure of the mixtures denser. The  $K_{ic}$  values for ACC specimens were higher than BC for all the UHPC mixtures.

**Table 4.9: Fracture toughness parameters for all the UHPC mixtures**

Curing Regime	Mixture ID	$P_{max}$ (kN)	$C_i$ (mm/kN)	$C_u$ (mm/kN)	$a_c$ (mm)	$K_{ic}$ MPa $\sqrt{m}$	$CTOD_c$ (mm)	$\delta_{max}$ (mm)
SC	M0	5.09	0.02210	0.05754	20.02	4.53	0.83053	2.784
	M1	4.44	0.02140	0.04601	18.65	3.83	0.48375	2.340
	M2	4.44	0.02477	0.04537	17.47	3.71	0.39741	2.340
	M3	4.37	0.02134	0.05950	20.50	3.93	0.78102	2.482
	M4	4.32	0.02604	0.06779	20.02	3.85	0.83060	2.492
	M5	4.26	0.02817	0.05366	17.76	3.59	0.47316	1.930
ACC	M0	4.58	0.02320	0.04928	18.56	3.94	0.52775	2.468
	M1	3.87	0.00775	0.04836	25.70	3.66	0.91826	2.794
	M2	3.79	0.02836	0.05126	17.38	3.15	0.37707	2.644
	M3	3.72	0.03360	0.04800	15.64	2.93	0.24155	3.064
	M4	3.48	0.04957	0.07718	16.27	2.80	0.42180	2.220
	M5	3.51	0.03526	0.04721	15.16	2.71	0.19635	2.522
BC	M0	3.46	0.03829	0.06400	16.80	2.83	0.38686	2.220
	M1	3.13	0.02716	0.04701	17.06	2.58	0.26994	3.170
	M2	3.41	0.04545	0.06116	15.19	2.64	0.24980	2.662
	M3	3.46	0.03974	0.06193	16.28	2.78	0.33707	2.220
	M4	3.42	0.02997	0.04386	15.82	2.71	0.21214	2.252
	M5	3.00	0.06083	0.06476	13.46	2.16	0.09396	2.810

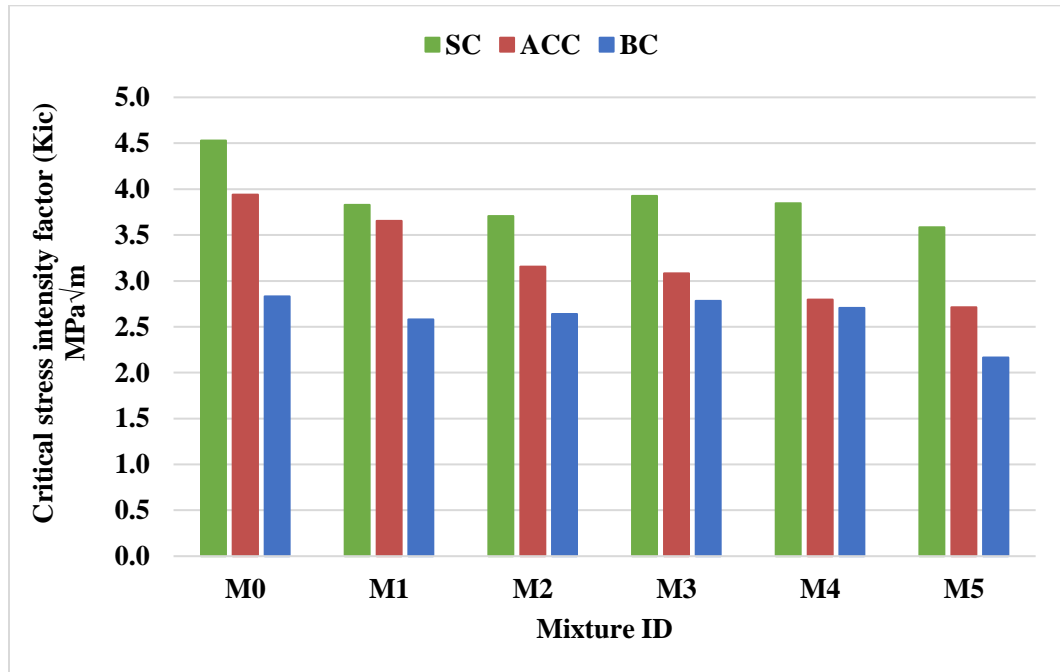


**Figure 4.15:  $K_{ic}$  values for all UHPC mixtures.**

The minor effect of the composition of mixtures can also be seen from the data in Figure 4.15. For example, a reduction in  $K_{ic}$  values due to the partial replacement of silica fume by natural pozzolan in mixtures M1 and M2 and partial replacement of Portland cement by natural pozzolan in the mixtures M3, M4 and M5.

## 4.8 Chloride Permeability

The rapid chloride penetration test (RCPT) is the most commonly method used to measure chloride permeability. ASTM C 1202 provides the procedures for this test as mentioned in the literature [52]. Based on the measured values of charges passing through concrete, the chloride permeability can be classified into five different categories, as presented in Table 4.10.

**Table 4.10: Different chloride permeability categories [52].**

Chloride permeability	Total charge (Coulombs)	Typical concrete type
High	> 4000	High w-c ratio (> 0.6) conventional PC concrete.
Moderate	2000 to 4000	Moderate w-c ratio (0.40 to 0.50) conventional PC concrete.
Low	1000 to 2000	Low w-c ratio (< 0.40) conventional PC concrete.
Very low	100 to 1000	Latex-modified concrete, internally sealed concrete.
Negligible	< 100	Polymer-impregnated concrete, polymer concrete.

The results of chloride permeability for all mixtures are presented in Table 4.11. Also, the plot of the chloride permeability values with its category classification are presented in Figure 4.16.



**Table 4.11: Chloride penetration results for all UHPC mixtures.**

Curing Regime	Chloride permeability (Coulombs)					
	M0	M1	M2	M3	M4	M5
SC	10	35	66	11	63	79
ACC	50	59	95	36	88	113
BC	59	61	119	65	106	136

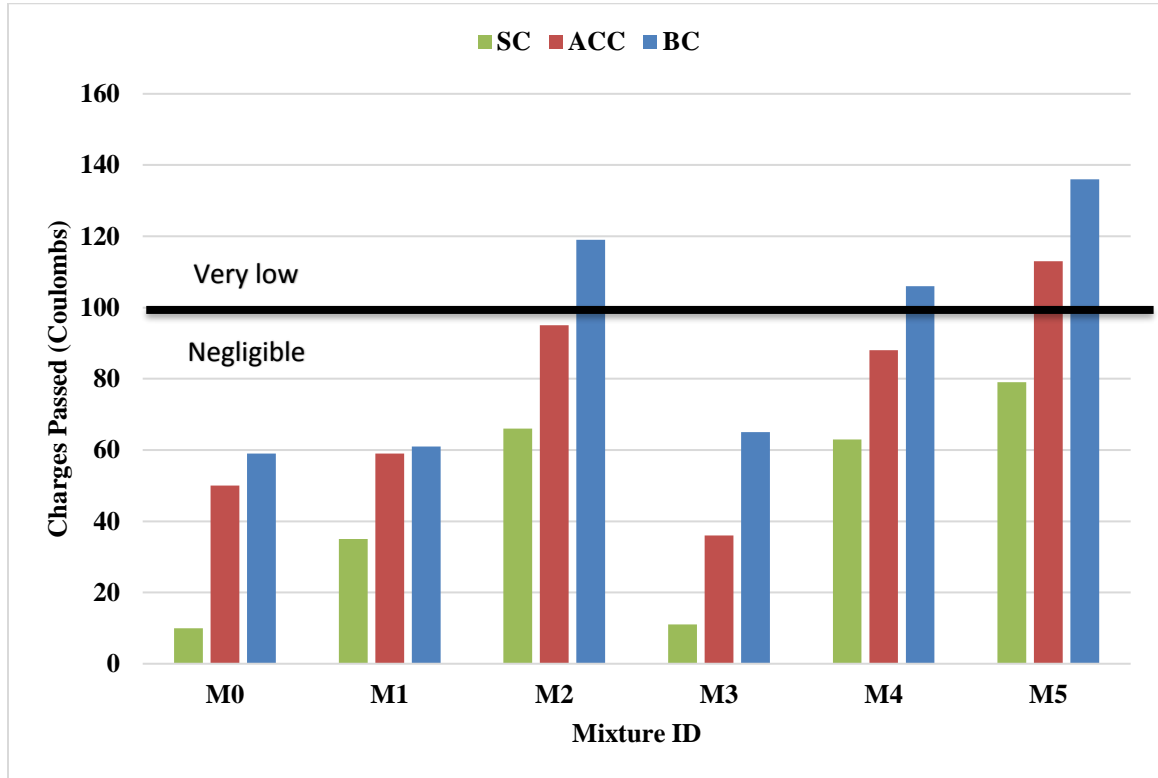


**Figure 4.16: Chloride permeability results for all mixtures.**

The data in Figure 4.16 indicate that all the mixtures subjected to SC have a ‘negligible’ chloride permeability. The same trend was observed for ACC, except the last mixture with 30% cement replacement by natural pozzolan, which has a ‘very low’ chloride permeability value (113 coulombs). It also shows that the specimens exposed to BC regime have the higher values of chloride permeability than those exposed to ACC, but still in a ‘very low’

chloride permeability category. It can be concluded that all the mixtures subjected to all three curing regimes have a very high resistance against reinforcement corrosion.

## **4.9 Drying Shrinkage**

The drying shrinkage strain for all the six UHPC mixtures treated with three curing regimes were conducted. Monitoring of drying shrinkage reading started directly after curing duration and it lasted up to 120 days of air curing. The average shrinkage values for each mixture were plotted in Figures 4.17 through 4.22. As usual, the shrinkage took place at a higher rate at early stages.

It can be observed from Figures 4.17 through 4.22 that for all UHPC mixtures, the shrinkage of specimens subjected to BC was lowest at any stage. The specimens subjected to ACC had highest shrinkage while the shrinkage for SC specimens was between that of ACC and BC. Higher shrinkage in case of ACC may be attributed to the chemical reactions due to carbonation process occurred on the concrete surface. However, as can be seen from Figure 4.23, the 7-day shrinkages for all six mixtures subjected all three curing regimes were found to be well below the maximum permissible 7-day shrinkage of 500 micro-strain. Further, it can be observed from Figure 4.24 that even the ultimate shrinkages (i.e., the steady state shrinkage after four months of exposure to air) for all six mixtures subjected all three curing regimes were found to be less than the maximum permissible 7-day shrinkage of 500 micro-strain, except the case of ACC where maximum ultimate shrinkage was recorded as 606 micro-strain that is not far away from permissible value.

It is evident from Figures 4.23 and 4.24 that the replacement of Portland cement and silica fume by natural pozzolan slightly reduced the shrinkage.

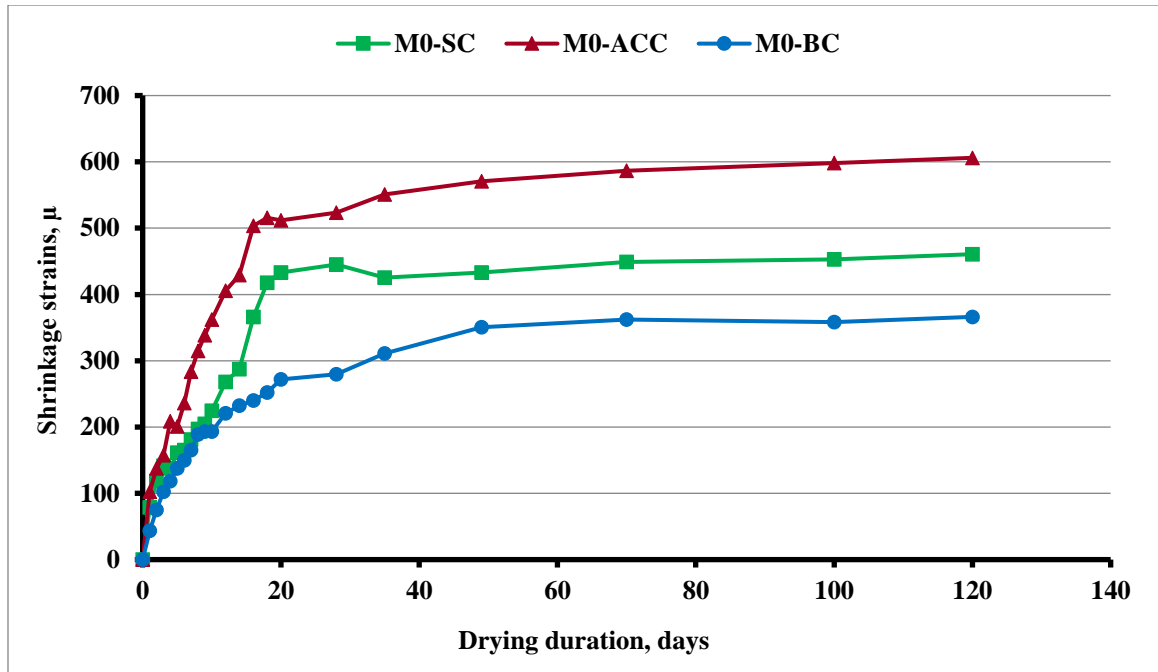


Figure 4.17: Drying shrinkage strain for mixture M0.

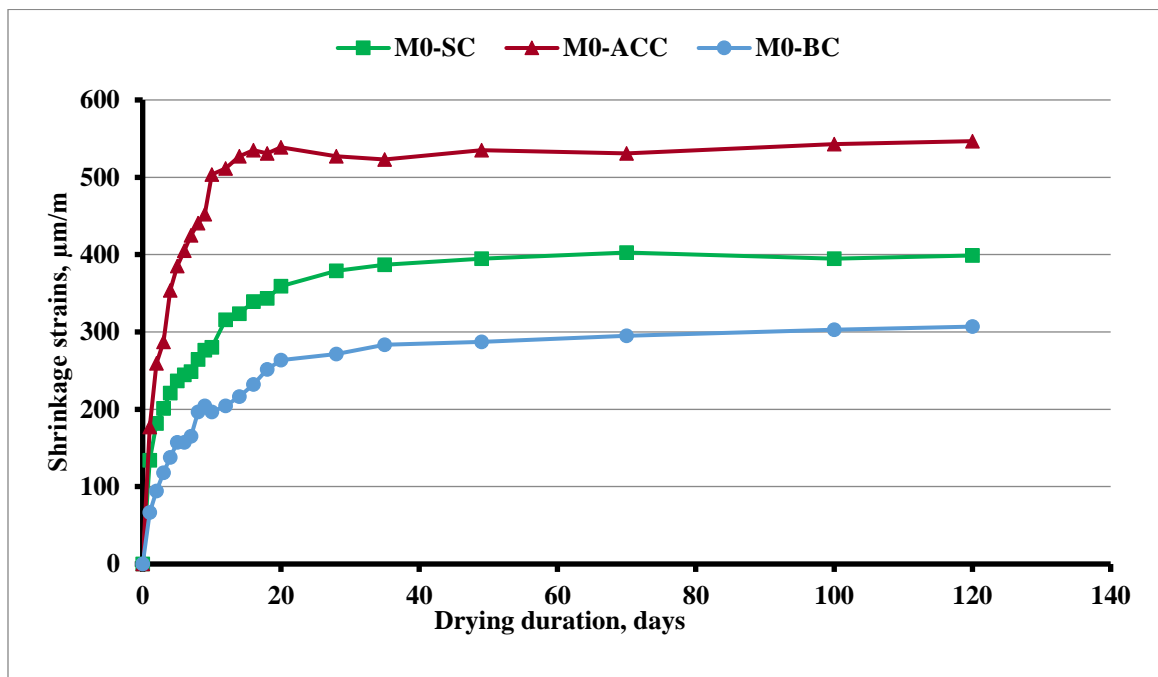


Figure 4.18: Drying shrinkage strain for mixture M1.

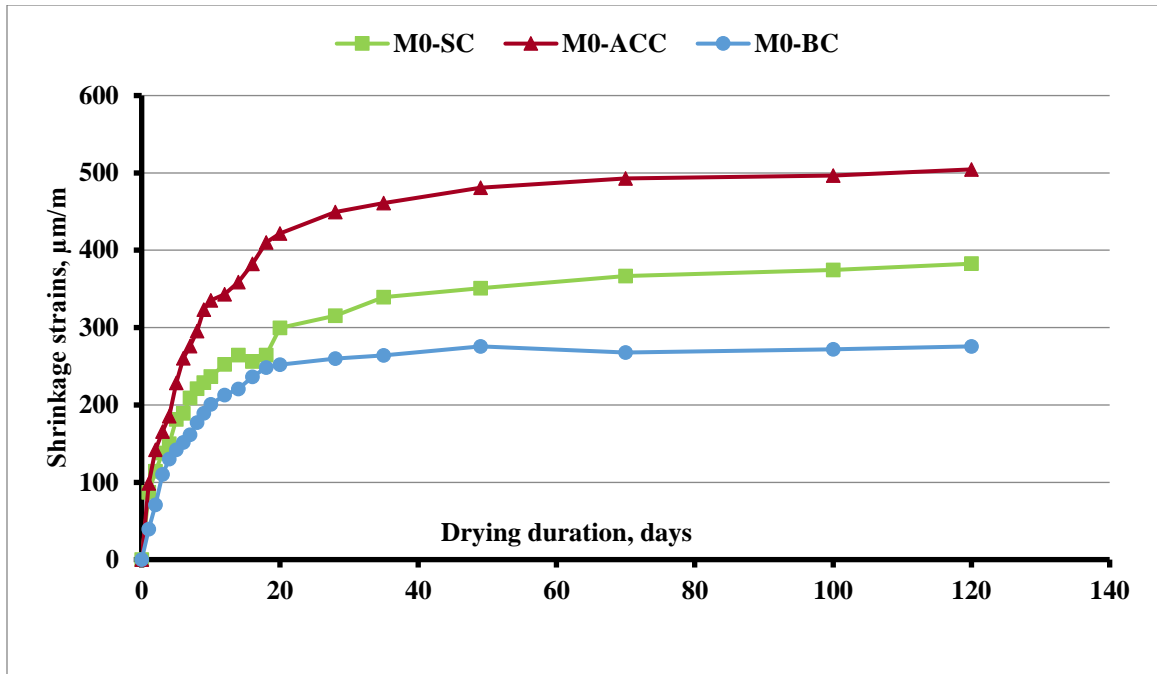


Figure 4.19: Drying shrinkage strain for mixture M2.

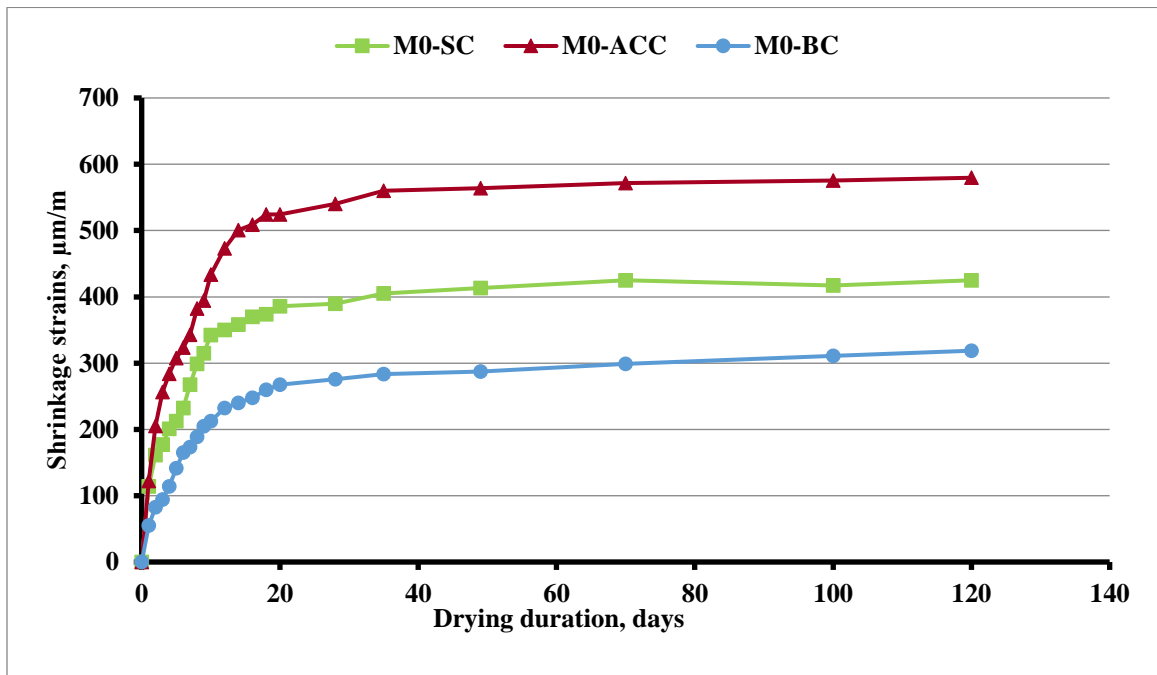


Figure 4.20: Drying shrinkage strain for mixture M3.

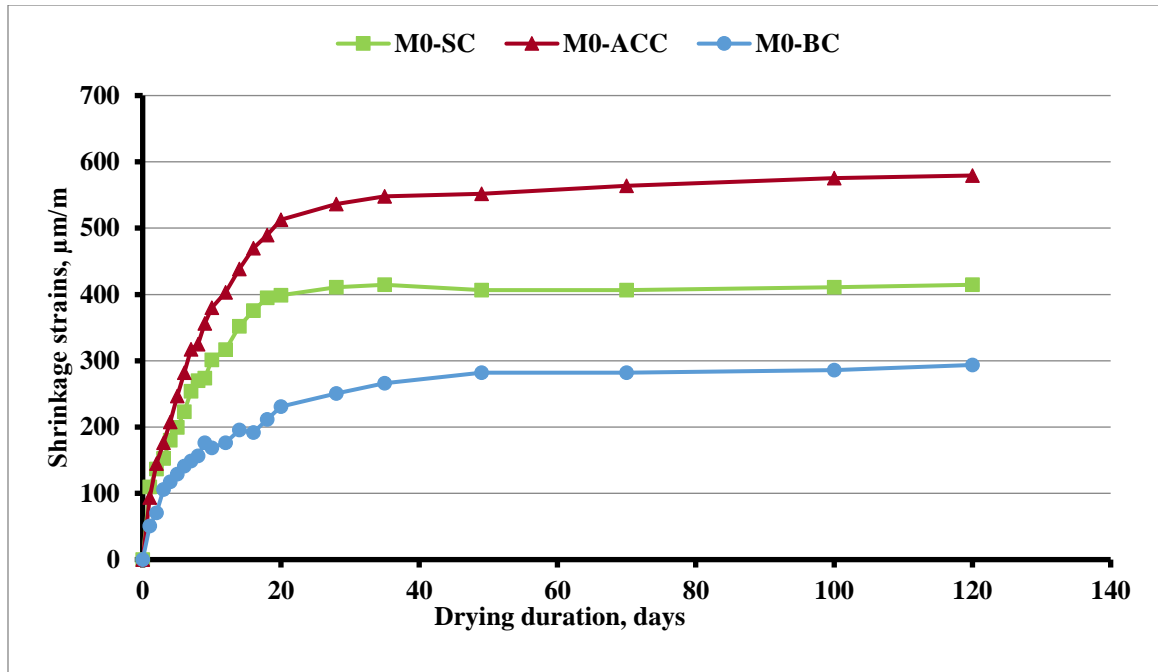


Figure 4.21: Drying shrinkage strain for mixture M4.

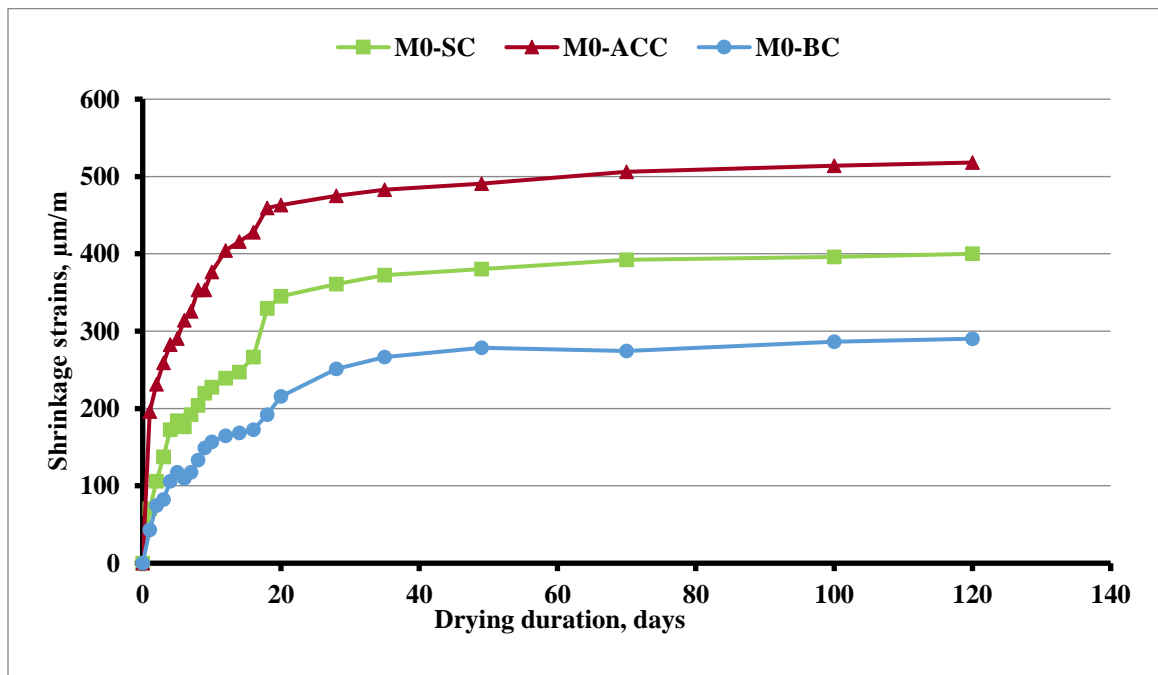


Figure 4.22: Drying shrinkage strain for mixture M5.

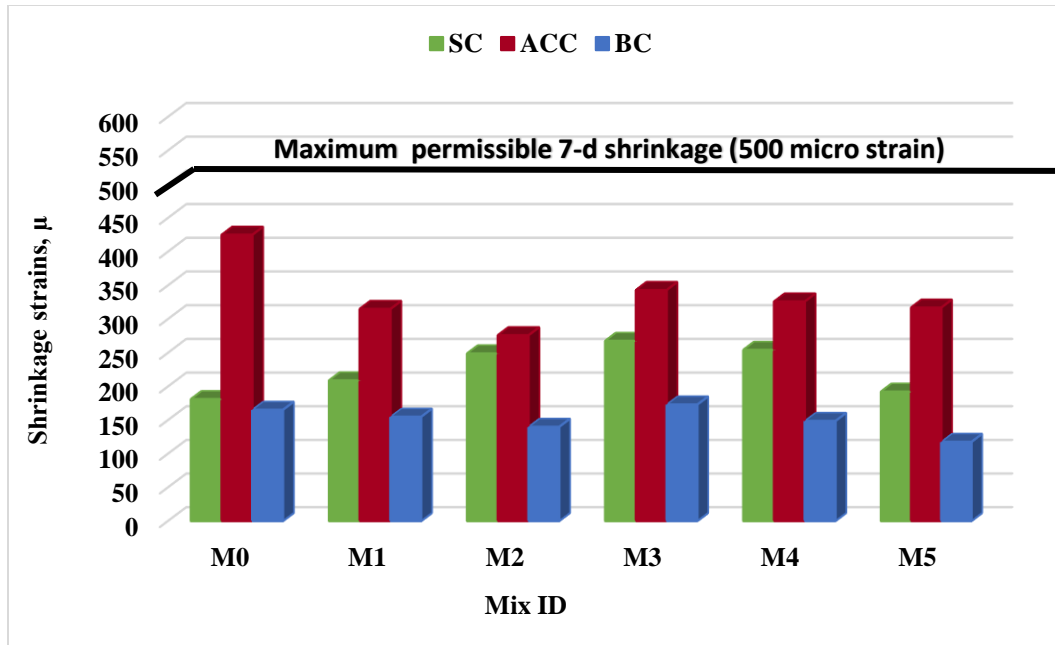


Figure 4.23: 7-days drying shrinkage readings

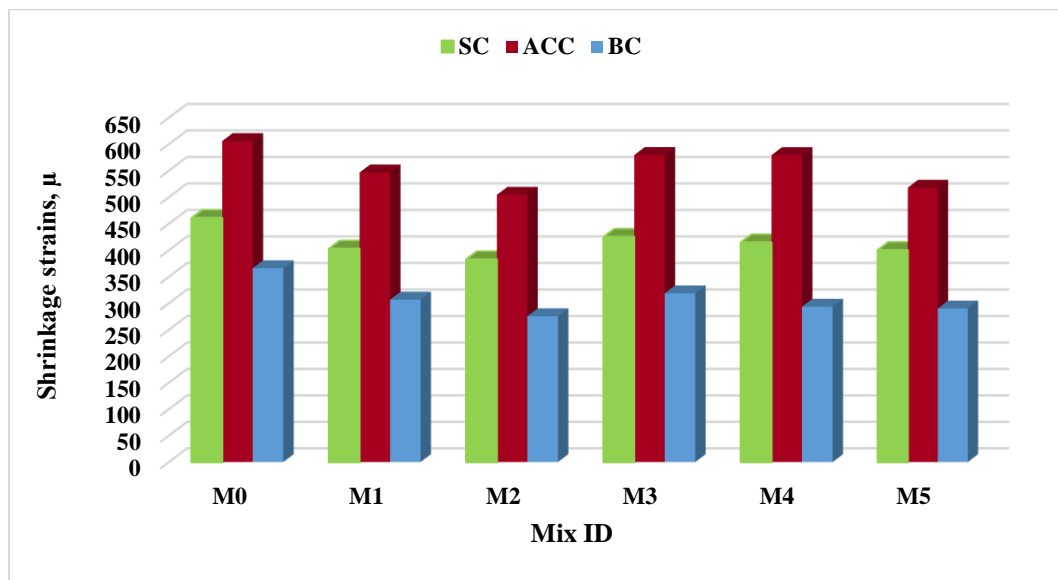


Figure 4.24: Ultimate Drying Shrinkage Values for All UHPC Mixtures

## 4.10 Scanning Electron Micrographs (SEM) and Energy-Dispersive X-ray Spectrographs (EDS)

In order to observe the effect of curing regime on the development of the microstructure and elemental composition, the scanning electron micrographs (SEM) and energy-dispersive X-ray spectrographs (EDS) of the reference mixture M0 cured with three curing regimes (SC, ACC, and BC) are typically shown in Figures 4.25 through 4.30, respectively.

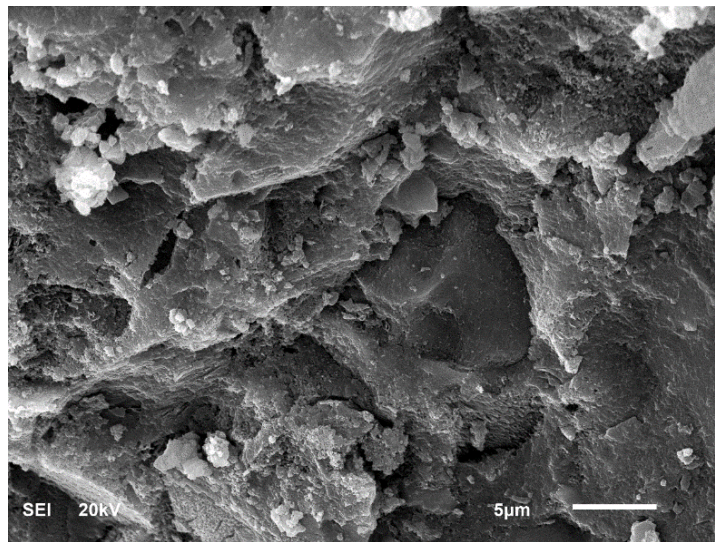


Figure 4.25: SEM micrograph of the mixture M0-SC.

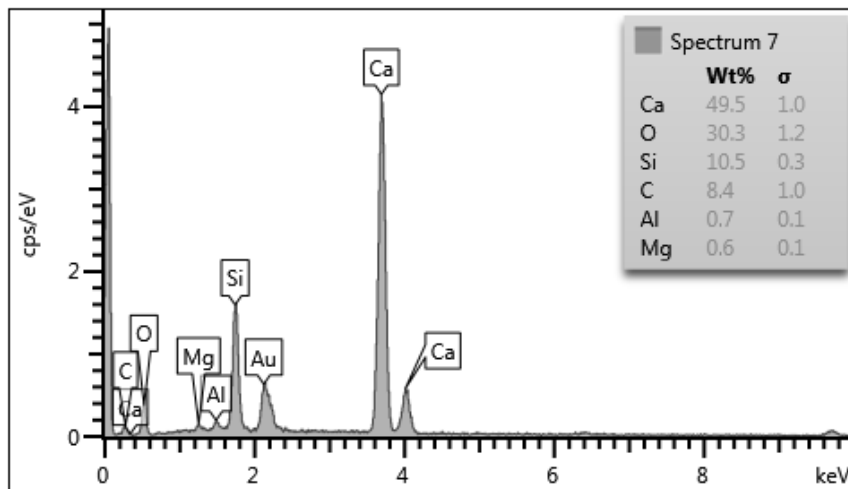
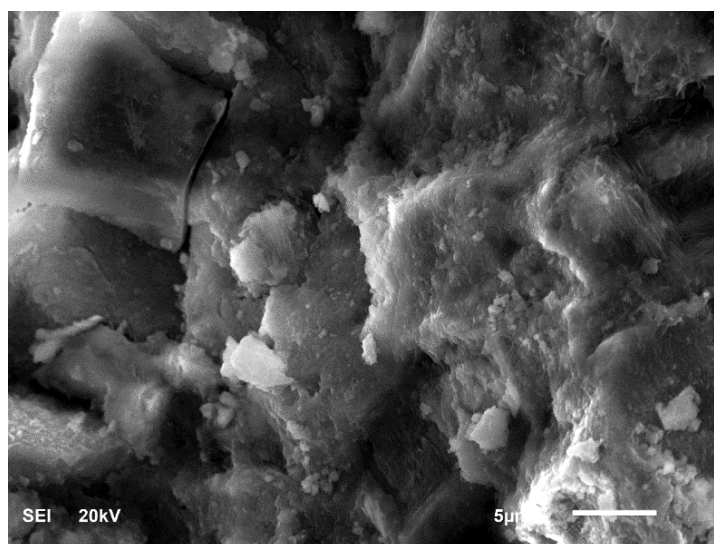
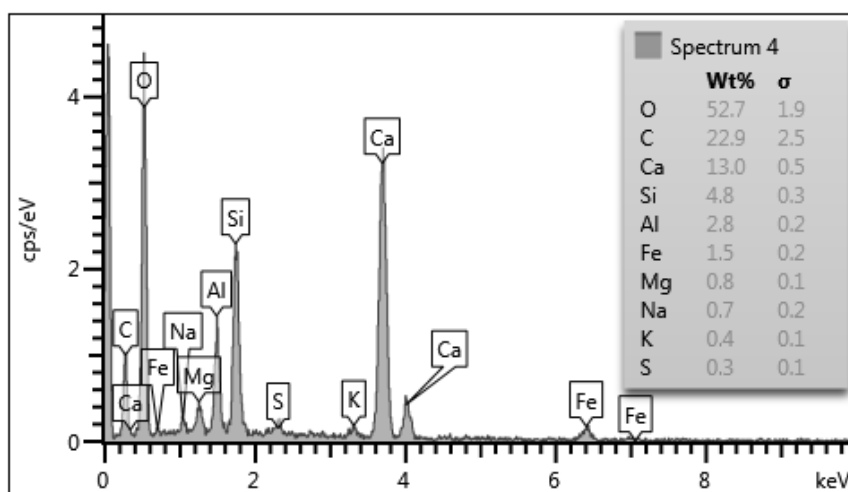


Figure 0.16: EDS of the mixture M0-SC



**Figure 4.27: SEM micrograph of the mixture M0-ACC.**



**Figure 0.28: EDS of the mixture M0-ACC**



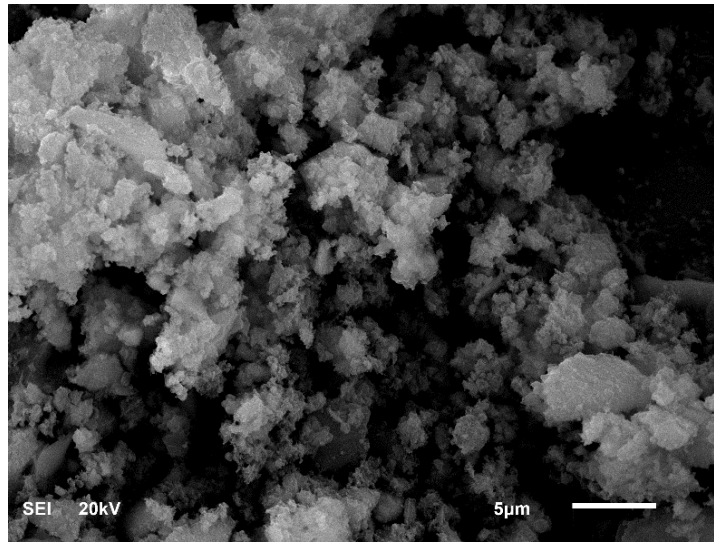


**Figure 4.29: SEM micrograph of the mixture M0-BC.**

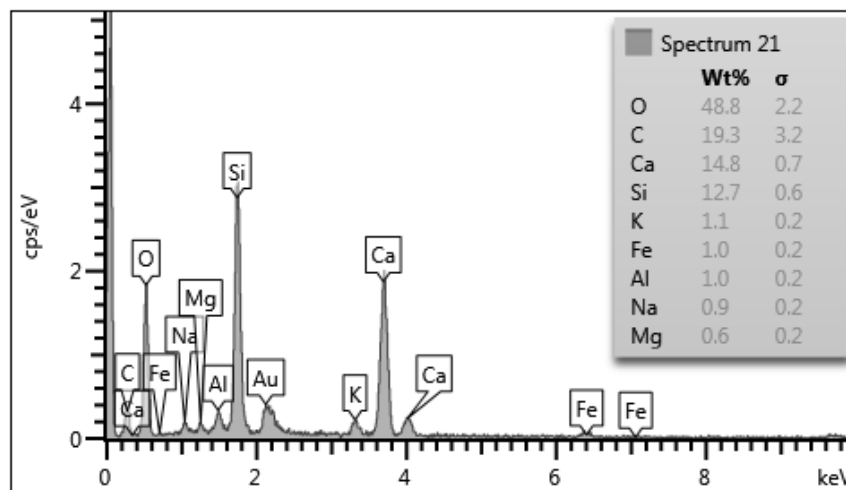


**Figure 0.30: EDS of the mixture M0-BC.**

For the mixture M0 subjected to SC, a dense microstructure was indicated in the SEM as indicated by high-resolution micrographs shown in Figure 4.25. The EDS of this specimen, as shown in Figure 4.26, indicates the presence of Ca (49.5%), Si (10.5%), and C (8.4%). Ca and Si are the elements generally found in Portland cement. The presence of Ca indicates minor carbonation of concrete due to the atmospheric carbon dioxide.

Figure 4.27 is the high-resolution SEM of mixture M0 cured by ACC. A dense microstructure is indicated due to the formation of  $\text{CaCO}_3$  on the surface of the specimen. The formation of  $\text{CaCO}_3$  crystal (hexagonal particle) is evident in Figure 4.27. The EDS spectrograph shown in Figure 4.28 shows the formation of mainly C (22.9%), Ca (13%) Si (4.8%), Al (2.8%) and other minor elements such as Fe, Mg, Na, K, and S. The increased quantity of carbon noted in this specimen indicates the formation of  $\text{CaCO}_3$ , which protects the inner C-S-H in the concrete.

Figure 4.29 showing the high-resolution SEM of mixture M0 cured by BC indicates a very porous microstructure. This shows that BC does not significantly improve the pore structure of concrete. The EDS shown in Figure 4.30 indicates the presence of C (19.3%), Ca (14.8%) Si (12.7%) and other minor elements such as Fe, Al, Mg, Na, and K. The presence of Ca in this specimen may be attributed to the formation of  $\text{CaCO}_3$  due to the reaction of atmospheric carbon dioxide with the  $\text{Ca}(\text{OH})_2$ . However, this reaction takes place at atmospheric pressure, thus the  $\text{CaCO}_3$  formed cannot fill up the pores in concrete and decrease its permeability.

## **CHAPTER 5**

### **CONCLUSIONS AND RECOMMENDATIONS**

#### **5.1 Conclusions**

Based on this exploratory study of different UHPC mixtures with different curing regimes, the following conclusions can be drawn:

1. The highest compressive strength was noted for SC regime. SC accelerates the hydration process due to heat treatment and moisture existence contribute to hydration of cement. About 75% of 28-days strength can be achieved with only 6 hours of SC.
2. The mixtures subjected to ACC and BC performed in a similar way with a slight difference between strength of ACC and BC specimens in the range of 0 to 3% after 28 days of air exposure.
3. Slightly higher early strength in ACC specimens than BC specimens was noted. The formation of  $\text{CaCO}_3$  layer at the surface of the ACC specimen significantly decrease the evaporation of the moisture from the core of the specimens allowing hydration of cement to continue which improved the properties over a long period of exposure to air.
4. Higher strength improvement noticed with SC regime with NP replacement, indicates that SC can be utilized to achieve an early high strength of UHPC with the addition of NP.
5. ACC curing regime improves the early age strength of concrete than BC. Moreover, the use of  $\text{CO}_2$  will lead to environmental protection. Therefore, ACC can be used in place of BC.

6. Like the case of compressive strength, all three curing regimes had similar effect on the other mechanical properties determined in this study that include splitting tensile strength, modulus of elasticity, and fracture toughness.
7. The shrinkage in case of ACC was highest and lowest in case of BC at all stages. However, all UHPC mixtures subjected to all three curing regimes had 7-day shrinkage well below the maximum permissible 7-day shrinkage of 500 micro-strain.
8. The chloride permeability was ‘negligible’ for most of the mixtures and a ‘very low’ for only last two mixtures with ACC and BC only. This indicates that the SC specimens have a denser microstructure than ACC and BC specimens. However, the low chloride permeability (‘negligible’ to ‘very low’) for all UHPC mixtures subjected to all curing regimes indicate a high resistance against reinforcement corrosion.
9. A dense microstructure was indicated in the SEM for SC and ACC specimens compared to the BC specimens.
10. It can be concluded finally that there is no significant effect of the change in the composition of the UHPC mixtures, particularly when they are exposed to air for long time after exposing to the curing regimes. Therefore, UHPC mixtures with the replacement of Portland cement by natural pozzolan up to 30% and replacement of silica fume up to 50% can be produced without compromising with the quality. This will save Portland cement and silica fume significantly.

## **5.2 Recommendations from this work**

1. A appropriate curing regime can be selected based on: (i) Strength required, (ii) Curing duration and (iii) Estimated cost needed.
2. Up to 30% NP till 30% can be replaced with cement or silica fume in UHPC mixtures.

3. ACC method is recommended for curing the precast concrete elements due to the following advantages:
  - a. High early compressive and tensile strength.
  - b. A small difference in strengths of ACC compared with BC specimens.
  - c. Mechanical properties and chloride permeability are comparable with BC.

### **5.3 Recommendations for future work**

1. Higher amount of NP replacement by cement or silica fume in UHPC mixtures.
2. Heat curing regime at higher temperatures.
3. Conducting other durability tests, such as reinforcement corrosion.

## REFERENCES

- [1] M. R. Moallem, "Flexural Redistribution in Ultra-High Performance Concrete Lab Specimens," Ohio University, 2010.
- [2] G. Yanni and V. Youssef, "Multi-scale investigation of tensile creep of ultra-high performance concrete for bridge applications," 2009.
- [3] Moon, Juhyuk, et al. "Characterization of natural pozzolan-based geopolymeric binders." *Cement and Concrete Composites* 53 (2014): 97-104
- [4] M. Shannag, "High strength concrete containing natural pozzolan and silica fume," *Cement and Concrete Composites*, vol. 22, pp. 399-406, 2000.
- [5] R. C. Mielenz, K. T. Greene, and N. C. Schieltz, "Natural pozzolans for concrete," *Economic Geology*, vol. 46, pp. 311-328, 1951.
- [6] G. K. Al-Chaar, M. Alkadi, and P. G. Asteris, "Natural pozzolan as a partial substitute for cement in concrete," *Open Construction and Building Technology Journal*, vol. 7, pp. 33-42, 2013.
- [7] T. Ahlborn, D. Harris, D. Misson, and E. Peuse, "Characterization of strength and durability of ultra-high-performance concrete under variable curing conditions," *Transportation Research Record: Journal of the Transportation Research Board*, pp. 68-75, 2011.
- [8] P. R. Prem, A. R. Murthy, and B. H. Bhaskar Kumar, "Influence of curing regime and steel fibres on the mechanical properties of UHPC," *Magazine of Concrete Research*, vol. 67, pp. 988-1002, 2015.
- [9] H. Patel, C. Bland, and A. Poole, "The microstructure of concrete cured at elevated temperatures," *Cement and Concrete Research*, vol. 25, pp. 485-490, 1995.

- [10] J. Jerga, "Physico-mechanical properties of carbonated concrete," *Construction and Building Materials*, vol. 18, pp. 645-652, 2004.
- [11] Y. Shao, X. Zhou, and S. Monkman, "A new CO<sub>2</sub> sequestration process via concrete products production," in *2006 IEEE EIC Climate Change Conference*, 2006, pp. 1-6.
- [12] V. Rostami, Y. Shao, and A. J. Boyd, "Durability of concrete pipes subjected to combined steam and carbonation curing," *Construction and Building Materials*, vol. 25, pp. 3345-3355, 2011.
- [13] V. Rostami, Y. Shao, A. J. Boyd, and Z. He, "Microstructure of cement paste subject to early carbonation curing," *Cement and Concrete Research*, vol. 42, pp. 186-193, 2012.
- [14] L. Mo and D. K. Panesar, "Effects of accelerated carbonation on the microstructure of Portland cement pastes containing reactive MgO," *Cement and Concrete Research*, vol. 42, pp. 769-777, 2012.
- [15] M. Schmidt and E. Fehling, "Ultra-high-performance concrete: research, development and application in Europe," *ACI Special publication*, vol. 228, pp. 51-78, 2005.
- [16] I. Y. Hakeem, "Characterization Of An Ultra-High Performance Concrete," May 2011.
- [17] Richard, Pierre, and Marcel Cheyrezy. "Composition of reactive powder concretes." *Cement and concrete research* 25.7 (1995): 1501-1511.
- [18] Ma J., Schneider H. (2002). Properties of Ultra-High-Performance Concrete, Leipzig Annual Civil Engineering Report (LACER), pp. 25-32.
- [19] Lubbers A.R. (2003). Bond performance between ultra high performance concrete and prestressing strands, MSc thesis, Ohio University.

- [20] Schmidt M., Fehling E. (2005). Ultra-high-performance concrete: research development and application in Europe, The 7th International Symposium on the Utilization of High-strength/High-performance concrete. American Concrete Institute, Washington DC, USA, SP 228-4, pp. 51-78.
- [21] Collepardi, S., et al. "Mechanical properties of modified reactive powder concrete." ACI Special Publications 173 (1997): 1-22.
- [22] F. de Larrard and T. Sedran, "Optimization of ultra-high-performance concrete by the use of a packing model," *Cement and Concrete Research*, vol. 24, no. 6, pp. 997–1009, 1994.
- [23] V. G. Papadakis, "Experimental investigation and theoretical modeling of silica fume activity in concrete," *Cement and Concrete Research*, vol. 29, no. 1, pp. 79–86, 1999.
- [24] K. Sobolev, "Th development of a new method for the proportioning of high-performance concrete mixtures," *Cement and Concrete Composites*, vol. 26, no. 7, pp. 901–907, 2004..
- [25] C. M. Tam, V. W. Y. Tam, and K. M. Ng, "Optimal conditions for producing reactive powder concrete," *Magazine of Concrete Research*, vol. 62, no. 10, pp. 701–716, 2010.
- [26] K. Wille, A. E. Naaman, and G. J. Parra-Montesinos, "Ultra-high performance Concrete with compressive strength exceeding 150 MPa (22 ksi): a simpler way," *ACI Materials Journal*, vol. 108, no. 1, pp. 46–54, 2011.
- [27] S. Ahmad, I. Hakeem, and M. Maslehuddin, "Development of an optimum mixture of ultra-high performance concrete", *European Journal of Environmental and Civil Engineering (France)*, Vol. 20, No. 9, pp. 1106-1126, 2016.
- [28] K. Ezziane, A. Bougara, A. Kadri, H. Khelafi, and E. Kadri, "Compressive strength of mortar containing natural pozzolan under various curing temperature," *Cement and Concrete Composites*, vol. 29, pp. 587-593, 2007.



- [29] W. Ma, D. Sample, R. Martin, and P. W. Brown, "Calorimetric study of cement blends containing fly ash, silica fume, and slag at elevated temperatures," *Cement, Concrete and Aggregates*, vol. 16, pp. 93-99, 1994.
- [30] M. J. Shannag and A. Yeginobali, "Properties of pastes, mortars and concretes containing natural pozzolan," *Cement and Concrete Research*, vol. 25, pp. 647-657, 1995.
- [31] Y. L. W. L Lam, C.S Poon, "Degree of hydration and gel/space ratio of high-volume fly ash/cement systems," *Cement and Concrete Research*, vol. 30 pp. 747–756, May 2000 2000.
- [32] S. Ahmad, I. Hakeem, and M. Maslehuddin, Development of UHPC mixtures utilizing natural and industrial waste materials as partial replacements of silica fume and sand. *Scientific World Journal*, 2014.
- [33] S. Kashef-Haghighi and S. Ghoshal, "Accelerated Concrete Carbonation: a CO<sub>2</sub> Sequestration Technology," in *8th World Congress of Chemical Engineering: Incorporating the 59th Canadian Chemical Engineering Conference and the 24th Interamerican Congress of Chemical Engineering, Montreal, QC, Canada*, 2009, p. 516.
- [34] C. D. Atiş, "Accelerated carbonation and testing of concrete made with fly ash," *Construction and Building Materials*, vol. 17, pp. 147-152, 2003.
- [35] Y. Shao, V. Rostami, Z. He, and A. J. Boyd, "Accelerated carbonation of portland limestone cement," *Journal of Materials in Civil Engineering*, vol. 26, pp. 117-124, 2013.
- [36] B. Zhan, C. Poon, and C. Shi, "CO<sub>2</sub> curing for improving the properties of concrete blocks containing recycled aggregates," *Cement and Concrete Composites*, vol. 42, pp. 1-8, 2013.

- [37] S. Monkman and Y. Shao, "Carbonation curing of slag-cement concrete for binding CO<sub>2</sub> and improving performance," *Journal of Materials in Civil Engineering*, vol. 22, pp. 296-304, 2009.
- [38] S. Kashef-Haghighi and S. Ghoshal, "Physico–Chemical Processes Limiting CO<sub>2</sub> Uptake in Concrete during Accelerated Carbonation Curing," *Industrial & Engineering Chemistry Research*, vol. 52, pp. 5529-5537, 2013.
- [39] J. Brooks and A. Al-Kaisi, "Early strength development of Portland and slag cement concretes cured at elevated temperatures," *Materials Journal*, vol. 87, pp. 503-507, 1990.
- [40] J. Escalante-Garcia and J. Sharp, "The microstructure and mechanical properties of blended cements hydrated at various temperatures," *Cement and Concrete Research*, vol. 31, pp. 695-702, 2001.
- [41] W. H. Mirza, S. I. Al-Noury, and W. H. Al-Bedawi, "Temperature effect on strength of mortars and concrete containing blended cements," *Cement and Concrete Composites*, vol. 13, pp. 197-202, 1991.
- [42] J. Dugat, N. Roux, and G. Bernier, "Mechanical properties of reactive powder concretes," *Materials and Structures*, vol. 29, pp. 233-240, 1996.
- [43] I. Hakeem, "Characterization of an ultra-high performance concrete," MS Thesis, King Fahd University of Petroleum & Minerals, Saudi Arabia, 2011.
- [44] B. A. Graybeal, "Material property characterization of ultra-high performance concrete," 2006.
- [45] A. Standard, "Standard test method for compressive strength of cylindrical concrete specimens," C39-86, pp. 20-24, 1997.
- [46] A. S. C469/C469M-10, "Standard Test Method for Static Modulus of Elasticity and Poisson's Ratio of Concrete in Compression," 2010.

- [47] C. ASTM, "496, Standard test method for splitting tensile strength of cylindrical concrete specimens," *ASTM International*, 1996.
- [48] H. Rüsch, D. Jungwirth, and H. K. Hilsdorf, *Creep and shrinkage: their effect on the behavior of concrete structures*: Springer Science & Business Media, 2012.
- [49] C. ASTM, "157/C 157M-06. Standard Test Method for Length Change of Hardened Hydraulic-Cement Mortar and Concrete," *Annual Book of ASTM Standards*, vol. 4.
- [50] S.-T. Kang, Y. Lee, Y.-D. Park, and J.-K. Kim, "Tensile fracture properties of an Ultra High Performance Fiber Reinforced Concrete (UHPFRC) with steel fiber," *Composite Structures*, vol. 92, pp. 61-71, 2010.
- [51] A. C. Bordelon, "Fracture behavior of concrete materials for rigid pavement systems," University of Illinois at Urbana-Champaign, 2007.
- [52] A. Standard, "C1202-12," *Standard test method for electrical indication of concrete's ability to resist chloride ion penetration. USA: ASTM International*, 2012.
- [53] D. Kyser, J. Hren, J. Goldstein, and D. Joy, "Introduction to analytical electron microscopy," *Plenum Press, New York*, 1979.

## VITAE

Name : Khaled Own Mohaisen  
Date of Birth : April 22, 1989  
Nationality : Palestinian  
Residential Address : Gaza-Palestine  
Email : khaled1136@hotmail.com

### EDUCATION

---

**Aug 2014 - Present    M.Sc. in Structural Engineering    (GPA 3.8 out of 4)**  
King Fahd University of Petroleum & Minerals - Saudi Arabia  
**Aug 2007 - Jan 2012    Bachelor Degree in Civil Engineering    (GPA 85 out of 100)**  
Islamic University of Gaza - Palestine

### EXPERIENCE

---

**Sep 2014 – Present    Teaching Assistant**  
King Fahd University of Petroleum & Minerals - Saudi Arabia  
**Dec 2012 - Aug 2014    Quality Control Engineer**  
BASHIR SIKSIK & CO. Company - Palestine  
**Dec 2011 - Dec 2012    Civil Engineer**  
ALMAQASED Co. for Engineering and Contracts - Palestine

### Memberships

---

American Concrete Institute Membership (ACI) No.: STU15-281.  
Association of Palestinian Engineers Membership No.: 9214